Peer-reviewed version available at Cancers 2018, 10, 269; doi:10.3390/cancers10080269

4-Acetyl-antroquinonol B suppresses SOD2-enhanced cancer stem cell-like phenotypes and chemoresistance of colorectal cancer cells by inducing hsa-miR-324 re-expression

Oluwaseun Adebayo Bamodu[1,2#], Ching-Kuo Yang[3#], David T.W. Tzeng[4], Kuang-Tai Kuo[5,6], Chun-Chih Huang[7], Li Deng[8,9], Hsiao M[10], Wei-Hwa Lee[11,12*], Chi-Tai Yeh[1,2*]

[1]Department of Hematology and Oncology, Cancer Center, Taipei Medical University - Shuang Ho Hospital, New Taipei City 23561, Taiwan. [2]Department of Medical Research & Education, Taipei Medical University - Shuang Ho Hospital, New Taipei City 23561, Taiwan. [3]Division of Colorectal Surgery, Department of Surgery, Mackay Memorial Hospital, Taipei City 110, Taiwan. [4] School of Life Sciences, The Chinese University of Hong Kong. [5]Division of Thoracic Surgery, Department of Surgery, School of Medicine, College of Medicine, Taipei Medical University, Taipei City 110, Taiwan. [6]Division of Thoracic Surgery, Department of Surgery, Shuang Ho Hospital, Taipei Medical University, New Taipei City 23561, Taiwan. [7]Department of Appiled Chemistry, Chaoyang University of Technology, Taichung, Taiwan. [8]Beijing Bioprocess Key Laboratory, College of Life Science and Technology, Beijing University of Chemical Technology, Beijing, China. [9]Amoy-BUCT Industrial Bio-technovation Institute, Amoy, China.[10]Genomics Research Center, Academia Sinica, Taipei, Taiwan. [11]Department of Pathology, Taipei Medical University - Shuang Ho Hospital, New Taipei City 23561, Taiwan; [12]Department of Pathology, School of Medicine, College of Medicine, Taipei Medical University, Taipei City 110, Taiwan.

# Contributed equally to this work

***** Corresponding Authors

Chi-Tai Yeh, Ph.D

Department of Medical Research and Education, Taipei Medical University - Shuang Ho Hospital, New Taipei City, Taiwan. Phone: +886-2-2490088 ext. 8881

FAX: 886-2-2248-0900; E-mail: ctyeh@s.tmu.edu.tw

Wei-Hwa Lee, M.D., Ph.D

Department of Hematology and Oncology, Taipei Medical University - Shuang Ho Hospital, New Taipei City, Taiwan. Phone: +886-2-2490088 ext. 8885

FAX: 886-2-2248-0900 ; E-mail: whlpath97616@s.tmu.edu.tw

Working title: 4-AAQB enhances chemosensitivity by inhibiting SOD2 and re-expressing hsa-miR-324-5p

Peer-reviewed version available at Cancers 2018, 10, 269; doi:10.3390/cancers10080269

Abstract

Background: Colorectal cancer (CRC) remains a leading cause of cancer-related morbidity and mortality in both sexes globally. This is not unconnected with the heterogeneity and plasticity of CRC stem cells (CRC-SCs) which stealthily exploit niche-related and (epi)genetic factors to facilitate metastasis, chemoresistance, tumor recurrence, and disease progression. Despite accumulating evidence of the role of dysregulated microRNAs in malignancies, the therapeutic efficacy of pharmacological-targeting of CRC-SC -associated microRNAs is relatively under-explored. **Experimental approach:** In this present study, we employed relatively new bioinformatics approaches, analyses of microarray data, western blot, RT-PCR, and functional assays to show that hsa-miR-324-5p expression is significantly suppressed in CRC cells, and inversely correlates with the aberrant expression of SOD2. **Results:** This converse hsa-miR-324-5p/SOD2 relationship is associated with enhanced oncogenicity, which is effectively inhibited by 4-AAQB as evidenced by inhibited cell viability and proliferation, as well as, attenuated migration, invasion and clonogenicity in 4-AAQB-treated DLD1 and HCT116 cells. We also showed that 4-AAQB-induced re-expression of hsa-miR-324-5p, akin to short-interfering RNA reduced SOD2 expression, correlates with the concurrent down-regulation of SOD2, N-cadherin, vimentin, c-Myc, and BcL-xL2, with concomitant up-regulation of E-cadherin and BAX2 proteins. Enhanced expression of hsa-miR-324-5p in the CRC cells suppressed their tumorigenicity *in vitro* and *in vivo*. Additionally, 4-AAQB synergistically potentiates FOLFOX anticancer effect by eliciting the re-expression of SOD2-suppressed hsa-miR-324 and inhibiting SOD2-mediated tumorigenicity. **Conclusion:** Our findings highlight the pre-clinical anti-CSC efficacy of 4-AAQB, with or without FOLFOX in CRC, and suggest a potential novel therapeutic strategy for CRC patients.

Keywords: 4-AAQB, SOD2, hsa-miR-324, colon cancer stem cells, chemoresistance, chemosensitivity

Peer-reviewed version available at Cancers 2018, 10, 269; doi:10.3390/cancers10080269

Highlights

- **i.** hsa-miR-324-5p expression is significantly suppressed in CRC cells
- **ii.** hsa-miR-321-5p inversely correlates with the aberrant expression of SOD2
- **iii.** 4-AAQB suppresses CSC-like phenotypes and enhance chemosensitivity
- **iv.** 4-AAQB elicits hsa-miR-324-5p re-expression in the CRC cells
- **v.** hsa-miR-324-5p re-expression suppressed CRC tumorigenicity and chemoresistance, *in vitro* and *in vivo*

Peer-reviewed version available at Cancers 2018, 10, 269; doi:10.3390/cancers10080269

1. Introduction

Colorectal cancer (CRC) is the third most commonly diagnosed malignancy and ranks as fourth leading cause of cancer-related deaths in both sexes, globally (1). In the US alone, diagnosis of over 95,500 and about 40,000 new cases of colon and rectal cancers, respectively, was predicted for the year 2017 (2). With a 5-year relative survival rate is ≥ 90% in stage I disease, and ~10% in stage IV disease, the therapeutic mainstay of CRC therapy remains surgery, neoadjuvant radiotherapy in rectal cases, and adjuvant chemotherapy for advanced stage and high-risk stage II colon cancer. (3).

Over the last decade, a decline in the incidence and mortality rates of CRC has been recorded in high-income countries; conversely, these rates continue to rise in low-resourced nations. This disparity in rates may be attributed to early screening, improved diagnostic techniques and better therapeutic strategies in the former, and senilization, increased embrace of western lifestyle, late diagnosis, excessive cost of conventional therapy in the later (4, 5), thus, necessitating the discovery and/or development of a relatively cheaper and more accessible therapeutic strategy. Similarly, the cumulative evidence of the presence and implication of a small subset of the CRC bulk termed CSCs in the tumorigenicity, oncogenicity, tumor progression, and disease recurrence of CRC (6, 7), further begs the case for a novel therapeutic option with CSC -targeting potentials, high curative efficacy and low drug-associated toxicity.

In an earlier work by our team, we demonstrated that 4-AAQB, a mycelial isolate of *Antrodia camphorata*, a common Taiwanese camphor tree mushroom with a broad range of documented bioactivities, effectively disrupts essential oncogenic signaling pathways such as the Lgr5/Wnt/β-catenin, JAK-STAT, and

non-transmembrane receptor tyrosine kinase signalling pathways, inhibits the acquisition of the CRC-CSC phenotype, down-regulates the expression and/or activities of stemness-associated genes including ALDH1, attenuates tumor aggression and accentuates chemosensitivity in CRC cells (8). Consistent with the growing evidence that microRNAs (miRNAs) are deregulated in several human cancer types including breast cancer, lung cancer, and colon cancer, potentially serving as screening and diagnostic factors (9, 10), as well as Leufkens et al.'s prospective cohort-nested case-control study (1064 CRC cases, 1064 matched controls), which provided evidence for the involvement of biomarkers of oxidative stress in the development of CRC (11), as a *sequela* to our previously published work, in this present study we continued exploring the therapeutic potential of 4-AAQB in CRC, particularly in the context of the probable regulatory role of 4-AAQB on the epigenetic landscape and modulation of oxidative stress in CRC.

In humans, the superoxide dismutase (SOD), with three subtypes, namely SOD1/ Cu,Zn-SOD, SOD2/Mn-SOD and SOD3/extracellular SOD, constitutes a principal component of the antioxidant defense system, also known as antioxidases. SOD2 is a 96 kDa homotetramer nuclear-encoded mitochondrial manganese (Mn)-containing antioxidant enzyme. Through its interaction with and binding to superoxide byproducts of oxidative phosphorylation, SOD2 is able to convert them into diatomic oxygen and hydrogen peroxide (H_2O_2). The Mn at the SOD2 active site catalyzes this disproportionization of superoxide anion to oxygen and H_2O_2, akin to SOD1 and SOD3 (12). Despite documented association between mutations in the SOD2 gene and several pathologies, including sporadic motor neuron disease, idiopathic dilated cardiomyopathy (IDC), premature aging (progeria) and cancer, the role of SOD2 in cancer cells, such as in CRC cells is not fully understood. While there are divergent

Peer-reviewed version available at Cancers 2018, 10, 269; doi:10.3390/cancers10080269

views on the actual role of SOD2 in cancer, there is growing evidence that the loss of SOD2 function may not facilitate metastatic disease progression as previously thought, rather there is indication from experimental and epidemiological studies that enhanced SOD2 expression levels correlates with metastatic malignantization and disease progression in various cancer types (13). It has been shown that the up-regulation of SOD2 protein expression is characteristic of certain cancers, including cervical and salivary adenoid cystic carcinoma (14, 15).

Deregulation of epigenetic factors and patterns, such as aberrant DNA methylation, histone tail modification and non-coding RNA (ncRNA) regulation, are implicated in loss of cell identity and contribute to several human pathologies, including cancer. Recent advances in the field of epigenetics are coupled with accumulating evidence of the critical role of non-coding RNAs, particularly miRNA expression and/or activity in oncogenicity (16). miRNAs are approximately 22 nucleotide (nt) long evolutionarily conserved small ncRNAs with the ability to elicit endogenous post-transcriptional silencing of its target genes based on complementarity with target sites in the 3′-untranslated regions (3′-UTRs) of the target gene/mRNA (16). There is documented correlation or association between down-regulated miRNA expression and tumor initiation or metastatic disease progression (17, 18), however, there is a dearth of information regarding SOD2-regulated miRNA(s) in CRC, and how the epigenetic modulation of SOD2 contributes to the CSC-like and metastatic phenotype of CRC cells.

Against the background of the conflicting data on SOD2 in malignancies, in this present study, we investigated the role of SOD2 in CRC, as well as, if and how 4-AAQB affects SOD2 expression profile in CRC. Additionally, considering the suggested cancer-related bivalence of SOD2, we also probed for probable epigenetic

undertone to SOD2-associated phenotype and likely SOD2-attenuating 4-AAQB therapeutic activity in CRC. Consequently, herein, we provide evidence that hsa-miR-324 interacts with SOD2, and that the aberrant expression of SOD2 enhances the oncogenicity and cancer stem cell-like phenotype of CRC cells and the therapeutic effect of 4-AAQB in these cells is mediated by inducing re-expression of SOD2-suppressed hsa-miR-324.

Peer-reviewed version available at Cancers 2018, 10, 269; doi:10.3390/cancers10080269

2. Materials and Methods

2.1. Reagents and Drugs

4-acetylantroquinonol B (4-AAQB, >99% purity) was purchased from New Bellus Enterprises Co., Ltd., Tainan City, Taiwan, while Leucovorin calcium (PHR1541 SIGMA-ALDRICH, 5-FU (F6627 SIGMA, ≥ 99% HPLC) and oxaliplatin (PHR1528 SIGMA-ALDRICH) were purchased from Sigma-Aldrich, Inc (St. Louis, MO, USA). Stock solutions of 10 mM in dimethyl sulfoxide (DMSO, Sigma-Aldrich) or sterile ddH_2O for 4-AAQB or FOLFOX, were stored at -20°C or 4°C, respectively, until use. Anti-SOD2 (ab13533 Rabbit pAb) antibody was purchased from Abcam plc. (Biochiefdom International Co., Ltd., New Taipei City, Taiwan), antibodies against E-cadherin (24E10: #3195, Rabbit mAb), N-cadherin (D4R1H: #13116, Rabbit mAb), and vimentin (D21H3: #5741, Rabbit mAb) were purchased from Cell Signaling Technology (CST, Beverly, MA, USA). Anti-c-Myc (9E10: sc-40), Oct4 (C-10: sc-5279), Sox2 (E-4: sc-365823), Bax (B-9: sc-7480), Bcl-xL (7B2.5: sc-56021), and β-actin (C4: sc-47778) antibodies were purchased from Santa Cruz Biotechnology (Santa Cruz, CA, USA). Alexa Fluor 647 donkey anti-rabbit IgG and Alexa Fluor 488 donkey anti-rabbit IgG were purchased from Invitrogen (Grand Island, NY, USA).

2.2. Cells and cell culture

The human non-tumor colon epithelial cell line FHC (ATCC-CRL-1831), as well as CRC cell lines DLD-1(ATCC-CCL-221) and HCT116 (ATCC-CCL-247) were purchased from the American Type Culture Collection (ATCC, Manassas, VA, USA), and cultured in DMEM/F-12 (Gibco™, 12-634-010), RPMI-1640 (Gibco™, 11-875-119) and McCoy's 5A modified (Gibco™, 16-600–082) medium, respectively. Both media were supplemented with 10% fetal bovine serum (FBS, Sigma, F7524)

Preprints (www.preprints.org) | NOT PEER-REVIEWED | Posted: 13 July 2018 doi:10.20944/preprints201807.0223.v1

Peer-reviewed version available at Cancers 2018, 10, 269; doi:10.3390/cancers10080269

and 1% penicillin-streptomycin (Gibco™, 15140) at 37ºC, in 5% humidified CO_2 incubator (Shel Lab, Sheldon Manufacturing, USA). Cells were sub-cultured at 90% confluence and the media changed every 72h.

2.3. Access and probe of online cancer data set

The Cancer Genome Atlas (TCGA) PANCANCER cohort dataset consisting of 14 cancer types were accessed and analyses of the expression profile of SOD2 and hsa-miR-324 in normal-cancer tissue pairs was performed using the the starBase v2.0 software algorithms (19). The TCGA colon cancer (COAD) cohort was also analyzed for the influence of SOD2 or hsa-miR-324 expression on survival rates.

2.4. miRNA profiling and secondary structure prediction

We used TargetScan (http://www.targetscan.org/), and miRANDA (http://www.microrna.org/microrna/home.do) for miR profiling and target sorting. The M-FOLD program v 2.3 The M-FOLD program (http://mfold.rna.albany.edu/?q=mfold) was used to predict the secondary structure of hsa-miR-324. The prediction was done as earlier described by Bellucci and colleagues (20).

2.5. Cell viability and drug combination assays

CRC cells were seeded in supplemented media at a density of 4×10^3 cells/well in triplicates in 96-well plates, incubated for 24 h in humidified 5% CO_2 at 37°C before exposure to different concentrations of the 4-AAQB for 48 h. Cell viability and/or

proliferation were assessed by sulforhodamine B (SRB, Sigma; 59012-5G) colorimetric assay following the manufacturer's instruction. Untreated wild-type cells served as control. Assay was performed three times in triplicates. Optical density (OD) was measured at 495 nm wavelength, using SpectraMax microplate reader (Molecular devices, Kim Forest Enterprises Co., Ltd, Taiwan).

2.6. Flow cytometry-based side population analysis.

To identify the CRC side population (SP), the DLD-1 or HCT116 cells were washed in warm RPMI-1640 media supplemented with 2% FBS and 10 mmol/L Hepes buffer (Invitrogen-Life Technologies, Carlsbad, CA, USA), re-suspended at a density of 1×10^6 cells per mL of RPMI-1640 supplemented with 2% FBS and 10 mmol/L Hepes buffer containing 5 µg/mL Hoechst 33342 dye, and incubated at 37°C for 1.5 h with gentle agitation. For the negative control, SP cells were incubated with 50 µM verapamil (Sigma-Aldrich), an ABC transporter inhibitor, washed with ice-cold Hank's balanced salt solution (HBSS) supplemented with 2% FBS and 10 mmol/L Hepes buffer, centrifuged, re-suspended in ice-cold supplemented HBSS. Cells were exposed to 1 µg/mL 7-Aminoactinomicin D (7-AAD, #A1310, Molecular Probes, Thermo Fisher Scientific Inc., Eugene, OR, USA) to delineate only viable cells. To obtain a single cell suspension, cells were filtered through a 70-µm filter, sorted into SP and non-SP cell fractions, then analyzed on the BD FACSAria II System (BD Biosciences, San Jose, CA, USA). Purity ≥ 98%.

Peer-reviewed version available at Cancers 2018, 10, 269; doi:10.3390/cancers10080269

2.7. Western blot analysis

Cultured CRC cells were harvested, washed thrice with PBS and lysate prepared using ice-cold lysis buffer solution. After being heated for 5 minutes, immunoblotting of the protein lysate was performed. Blots were blocked for 1 h with 5% skimmed milk in TBST, incubated overnight at 4°C with specific primary antibodies against SOD2 (1:1000), E-cadherin (1:2000), N-cadherin (1:2000), vimentin (1:1000), c-Myc (1:1000), BAX (1: 1000), BCL-xL (1: 1000), and β-actin (1:500). Thereafter, the polyvinylidene difluoride (PVDF) membranes were washed three times with TBST, then incubated with horseradish peroxidise (HRP)-labeled secondary antibody for 1h at room temperature and washed with TBST again before band detection using the enhanced chemiluminescence (ECL) Western blotting reagents and imaging with the BioSpectrum Imaging System (UVP, Upland, CA, USA).

2.8. miRNA and small interfering RNA (siRNA) transfection

For miRNA transfection, micrON^{TM} hsa-miR-324-5p mimic (#miR10000761-1-5), micrOFF^{TM} hsa-miR-324-5p inhibitor (#miR20000761-1-5), micrON^{TM} mimic negative control #22 (# miR01101-1-5) and micrOFF^{TM} inhibitor negative control #22 (#miR02101-1-5) were purchased from RiboBio (Guangzhou RiboBio Co. Ltd, Guangzhou, China). For transient silencing of SOD2, the SOD2-specific siRNA (si-h-SOD2_001, B000006648A-1-5) were also purchased from RiboBio (Guangzhou RiboBio Co. Ltd, Guangzhou, China). Lipofectamine 2000 (Invitrogen, Carlsbad, CA, USA) was used for the transfection of the miRNA oligonucleotides and siRNA following the manufacturer's protocol. The total RNA or protein were extracted 48 h after transfection and used for the RT-PCR or western blot analyses.

Peer-reviewed version available at Cancers 2018, 10, 269; doi:10.3390/cancers10080269

2.9. Scratch wound healing assay

Cell migration potential was evaluated using the wound healing assay. Briefly, DLD-1 or HCT116 cells were seeded onto 6-well plates (Corning Inc., Corning, NY, USA) with complete growth media containing 10% FBS and cultured to 99-100% monolayer confluency. The cell monolayers were scratched with a sterile yellow pipette tip to denude the culture wells. The cell migration images were captured at the 0 and 24 h time points after denudation, under microscope with 10X objective lens and analyzed with the NIH ImageJ software (https://imagej.nih.gov/ij/download.html).

2.10. Transwell matrigel invasion assay

Using the 24-well plate Transwell matrigel invasion system, 3×10^4 DLD-1 or HCT116 cells were seeded into the upper chambers of the inserts (BD Bioscience, 8μm pore size) containing FBS-free media with different concentration of 4-AAQB and media containing 10 % FBS in the lower chamber served as chemo-attractant. After 24 h cell incubation, media were discarded; cells on filter membrane were fixed with 3.7 % formaldehyde for 1 h, and then stained with 0.2% (w/v) crystal violet solution, for 15 min, while cells on the upper side of the inserts were gently removed with cotton swab. The invaded cells were visualized, and invasive capacity was evaluated as the total number of cells on the lower surface of the membrane, as determined by microscopy.

2.11. Colony formation assay

2×10^4 DLD-1 or HCT116 cells were plated into 6-well cell culture plates (Corning Inc., Corning, NY, USA) and incubated for 2 weeks at 37°C after treatment with

Peer-reviewed version available at Cancers 2018, 10, 269; doi:10.3390/cancers10080269

different concentrations of 4-AAQB. Then, cells were washed thrice with PBS, fixed with ice-cold methanol, stained with 0.005 % crystal violet, washed with PBS and dried at room temperature. Formed colonies were then assessed and counted under microscope. In each well, the total number of colonies with diameter ≥ 100 µm was counted over 6 randomly selected fields in triplicate assays.

2.12. Tumorsphere and clonal tumorsphere formation assay

5×10^3 DLD-1 or HCT116 cells were plated per well containing stem cell media with different concentrations of 4-AAQB in ultra-low attachment 6-well plates (Corning Inc., Corning, NY, USA) in quadruplicate. The stem cell media consisted of serum-free growth media, supplemented with 1X B27 supplement, 10 ng/ml human basic fibroblast growth factor (bFGF; (Invitrogen, Grand Island, NY, USA) and 20 ng/ml epidermal growth factor (EGF; (Invitrogen, Grand Island, NY, USA), and was changed every 72 h. After 12 days of culture, primary colonospheres consisting of ≥20 cells were counted, and images acquired. Secondary colonospheres were generated by dissociating primary colonospheres by trysinization and pippetted through a 22G needle to obtain a single-cell suspension (Thermo Fisher Scientific Inc.). After dissociation of the primary tumorspheres, cell seeding and exposure to 4-AAQB was akin to that for primary tumorspheres.

2.13. Immunohistochemistry and Immunofluorescence Staining

Immunohistochemical (IHC) analyses of the Taipei Medical University - Shuang Ho Hospital CRC cohort consisting of different tumor stage colorectal cancer specimens with different clinical stages was performed. Recommendations of the Declaration of

Peer-reviewed version available at Cancers 2018, 10, 269; doi:10.3390/cancers10080269

Helsinki for biomedical research involving human subjects were followed. Ethical approval for the study was obtained from Joint Institutional Review Board of the Taipei Medical University (approval number: N201602054). A review of patients' clinical records to determine tumor stage at the time of diagnosis and outcome was carried out. Antibody against SOD2 (1:200, ab13533 Rabbit pAb) was used in accordance to standard IHC procedure. SOD2 expression was evaluated and scored by 2 independent pathologists using the quick-score (Q-score) based on the staining intensity (I) and stained cells percentage (P). Staining intensity was defined as 0 (no staining), 1+ (weak), 2+ (moderate) and 3+ (strong). $Q = I \times P$ where maximum score was 300. For the immunofluorescence (IFC) staining, untreated or 4-AAQB-treated DLD-1 or HCT116-derived colonospheres were plated onto poly-L-lysine-coated glass cover-slips, fixed with 4% paraformaldehyde, and carefully washed thrice with PBS. This was followed by cell permeabilization with 0.1% Triton X-100/PBS solution for 10 min and incubation with primary antibodies against Oct-4 and Sox2 (Santa Cruz, CA, USA), then with goat anti–mouse Alexa Fluor488 secondary antibody (Cat. #: R37120, Thermo Fisher Scientific Inc.). Cell nuclei were labeled with DAPI (4',6-diamidino-2-phenylindole; Cat. #: D1306, (Molecular Probes, Thermo Fisher Scientific Inc., Eugene, OR). Cell visualization and imaging was done using the Nikon E800 fluorescent microscope.

2.14. RNA extraction, Real-time polymerase chain reaction (RT-PCR)

Total RNA was isolated from the CRC cell line DLD-1 and resected xenograft tumor sample, using the RNeasy kit (Qiagen Inc., MD, USA). The miRNEasy kit (Qiagen) was used for miRNA purification. Total RNA concentration was determined using NanoDrop ND1000 spectrophotometer (Nyxor Biotech, Paris). The PCR mixtures

Preprints (www.preprints.org) | NOT PEER-REVIEWED | Posted: 13 July 2018 doi:10.20944/preprints201807.0223.v1

Peer-reviewed version available at Cancers 2018, 10, 269; doi:10.3390/cancers10080269

were prepared using the SYBR Green Master Mix (Applied Biosystems, Life Technologies, Grand Island, NY, USA). The PCR contained the primers, the fluorogenic probe mix, and the TaqMan Universal PCR Master mix (Applied Biosystems, CA, USA). Amplification reactions were performed in triplicate from 20 ng cDNA using the Bio-Rad C1000 real-time PCR system (Bio-Rad, Cambridge, MA, USA) using the following condition: 95°C for 3 min, 35 cycles at 95°C for 15 sec, 60°C for 30 sec, 72°C for 30 sec, and 72°C for 10 min. Results were analyzed and all values were normalized to the levels of the housekeeping gene β-actin, which served as the internal control. All procedures were in accordance to the manufacturers' instructions. The PCR primer sequence are as follows: SOD2 (forward): 5′-GCCTCCCTGACCTGCCTTAC-3′, (reverse): 5′-GTGATTGATATGGCC CCCG-3′; hsa-miR-324-5p (forward): 5'-CGCGGATCCGGGTGGAT GTAAGGGATGAG-3'; (reverse): 5'-CCGGAATTCTTGGGCT GATCCAGGAGAAG-3'; and β-actin (forward): 5′-CCCTAAGGCCAACCGTGAA-3′, (reverse): 5′-CCAGAGGCATACAG GGACAAC-3′

2.15. Oral administration of 4-AAQB in vivo and primary tumor experiments

Severe immune comprised NOD/SCID mice (6 weeks old) were purchased from BioLASCO (Taipei, Taiwan) and housed in Memorial Hospital Animal Center under SPF conditions. All the animal experiments were performed under the strict adherence to the regulations set by MacKay Memorial Hospital Animal Center (Approved protocol number: MMH-104-024). The mice were bred and maintained in pathogen-free conditions, with sterile water and feed, in air-controlled rooms with specifically designed 12 h light/dark cycle. 1 x 10^5 DLD-1 cells suspended in 100 μL PBS was injected subcutaneously into the right flank of 6 - 8-week-old, female

Preprints (www.preprints.org) | NOT PEER-REVIEWED | Posted: 13 July 2018 doi:10.20944/preprints201807.0223.v1

Peer-reviewed version available at Cancers 2018, 10, 269; doi:10.3390/cancers10080269

NOD/SCID mice (n = 5/treatment group; average body weight, 22.5±3.74 g). Tumor growth was monitored daily and tumor size measured every 48 h with callipers based on the formula: $\left(x * y^2\right)/2$, where x = longest diameter, and y = diameter perpendicular to x. When tumors became palpable (~ 50-150mm^3) on day 7-8 after inoculation, the mice were randomly assigned to treatment groups, with oral administration of vehicle (100 mL - 50 mM PBS), 4-AAQB (n = 5; 5 mg/kg q48h), FOLFOX (n = 5; 15 mg/kg 5-FU q24h, 5 mg/kg folinate q24h and 5 mg/kg oxaliplatin q1wk) or 4-AAQB + FOLFOX (n= 5), for five weeks. Tumors were resected and weighed after humane sacrifice of the mice. The feeding habit, motor activity and body weight of the mice were all monitored as indicators of murine general health. Analysis of variance (ANOVA) was used to establish differences between groups, and significance levels were determined by non-parametric Kruskal-Wallis test.

2.16. Statistical analysis

All assays were performed at least thrice in triplicates. Values are expressed as mean ± standard error of mean (SEM). Comparison between two groups was estimated using the 2-sided Student's t-test, while the one-way analysis of variance (ANOVA) was used for comparison between 3 or more groups. All statistical analyses were performed utilizing the GraphPad Prism 5 software (GraphPad Software Inc., La Jolla, CA, USA). P-value < 0.05 was considered statistically significant.

3. Results

3.1. A reciprocal down-regulation of SOD2 and hsa-miR-324-5p gene expression exists in various human cancer types, including CRC cells

To characterize the role of SOD2 in human cancer, we examined the expression profile of SOD2 in matched pairs of tumor and adjacent non-tumor tissues in 14 different human cancer types from the cancer genome atlas (TCGA) PANCANCER dataset with SOD2 data (n = 5599). Compared to its expression in adjacent non-tumor tissues, hsa-miR-324-5p expression was significantly down-regulated in bladder urothelial carcinoma (BLCA, ~0.53-fold), breast invasive carcinoma (BRCA, ~0.5-fold), head and neck squamous cell carcinoma (HNSC, ~0.83-fold), kidney chromophobe cell carcinoma (KICH, ~0.77-fold), lung adenocarcinoma (LUAD, ~0.77-fold), lung squamous cell carcinoma (LUSC, ~0.55-fold), and thyroid carcinoma (THCA, ~0.91-fold), but conversely, up-regulated in colorectal cancer (CRC, ~1.0-fold), kidney renal clear cell carcinoma (KIRC, ~2.2-fold), and uterine corpus endometrial carcinoma (UCEC, ~1.1-fold), while no comparative non-tumor data was available for glioblastoma (GBM), acute myeloid leukemia (LAML), ovarian carcinoma(OV),and skin cutaneous melanoma (SKCM) (**Figure 1A**). The SOD2 expression data for CRC was corroborated by that obtained from analysis of the TCGA CRC dataset (n = 237) using the Oncomine platform (https://www.oncomine.org), with a 8.47-fold (n =22, p = 5.55E-10), 1.93-fold (n = 101, p = 1.92E-13), 1.88-fold (n = 60, p = 2.88E-10) and 1.45-fold (n = 6, p = 6.25E-4) up-regulation of SOD2 expression level was observed in the colon mucinous adenocarcinoma, colon adenocarcinoma, rectal adenocarcinoma, and rectal mucinous adenocarcinoma compared to the non-tumor 'normal' colorectal tissues (**Figure 1B**). Furthermore, we employed a bioinformatics approach to systematically screened for

miRNAs that interact with SOD2, sorted them out by interaction propensity, sequence complementarity, and broad conservation across species based on data from TargetScanHuman release 7.1 (http://www.targetscan.org/vert_71/) and miRanda (http://www.microrna.org/ microrna/). We observed high interaction propensity, broad conservation and good complementarity between the 5' end of hsa-miR-324-5p and the 3' end of SOD2. In parallel analyses of the TCGA datasets, in comparison with SOD2, we observed a reciprocity in the expression profile of hsa-miR-324-5p for CRC and KIRC only in the miRNA-relevant PANCANCER dataset (n = 5613); such that hsa-miR-324-5p was significantly suppressed in CRC (~0.26-fold), KIRC (~0.77-fold), GBM (~0.48-fold) , KICH (~0.50-fold), and THCA (~0.91-fold) compared to the non-tumor tissue group, but enhanced in BLCA (~5.2-fold), BRCA (~1.2-fold), HNSC (~2.8-fold), LUAD (~2.7-fold), SKCM (~6.8-fold) and UCEC (~4.1-fold), while no comparative non-tumor data was provided for glioblastoma (GBM), acute myeloid leukemia (LAML), ovarian carcinoma (OC),and skin cutaneous melanoma (SKCM), while no comparative non-tumor data was available for LAML and OV (**Figure 1C**). As with SOD2 expression, the hsa-miR-324-5p expression data for CRC in the PANCANCER cohort was consistent with data obtained from analysis of the TCGA CRC dataset (n = 325), with a markedly down-regulated hsa-miR-324-5p expression level in the CRC compared to the non-tumor colorectal tissues (0.26-fold, $p = 1.03 \times 10^{-13}$) (**Figure 1D**). This finding, at least in part, is indicative of the tumor-promoting role of reciprocal down-regulation of SOD2 and hsa-miR-324-5p gene expressions in various human cancer types, including CRC cells.

Peer-reviewed version available at Cancers 2018, 10, 269; doi:10.3390/cancers10080269

3.2. SOD2 interacts directly with and suppresses hsa-miR-324 expression in CRC cells.

To better understand the relationship between SOD2 and hsa-miR-324-5p, as well as rule out any modulatory loop between them in CRC cells, we employed a bioinformatics approach to generate the crystal structure of SOD2 based on PDB:2ADQ from the Protein Data Bank (www.rcsb.org/pdb/gene/SOD2; **Figure 2A**). For visualization of our hypothesized molecular interaction between hsa-miR-324-5p and SOD2, we generated the tertiary (3D) structure of hsa-miR-324-5p from its sequence-derived 'brackets and dots' linear structure and minimum free energy (MFE) secondary (2D) structure (**Figure 2B**). We then used the EduPyMoL molecular interaction and visualization software to demonstrate the interaction between SOD2 and hsa-miR-324-5p, observing high interaction propensity, broad conservation and good complementarity between the 5' end of hsa-miR-324-5p and the 3' end of SOD2, demonstrated by a shape complementarity/docking score of 14236, atomic contact energy (ACE) of -33.40, a solvation folding energy of -18.60 Kcal/mol, an approximate SOD2-hsa-miR-324 complex interface area of 1896.30, when a root mean square distance (RMSD) of 9 is used for the final docking, and a p-value of 2.08×10^{-3} (**Figure 2C**). Moreover, to demonstrate that the observed SOD2 - hsa-miR-324 interaction was modulatory in nature, we transfected the human CRC cell line DLD-1 with hsa-miR-324 negative control (NC), mimic or inhibitor. We observed significant down-regulation in the SOD2 protein expression following transfection of the DLD-1 cells with the hsa-miR-324 mimic, compared to the mimic NC-transfected cells (0.24-fold; $p < 0.01$). Conversely, transfection with hsa-miR-324 inhibitor elicited marked up-regulation of SOD2 protein expression level, in comparison with the inhibitor NC-transfected cells (6.8-fold; $p < 0.001$) (**Figure 2D**).

Preprints (www.preprints.org) | NOT PEER-REVIEWED | Posted: 13 July 2018 doi:10.20944/preprints201807.0223.v1

Peer-reviewed version available at Cancers 2018, 10, 269; doi:10.3390/cancers10080269

These findings indicate that SOD2 interacts directly with and suppresses hsa-miR-324 expression in CRC cells.

3.3. Aberrant expression of SOD2 correlates with disease progression and SOD2-induced down-regulation of hsa-miR-324 facilitates poor prognosis.

With an intention to establish a connection between the expression profiles of SOD2, hsa-miR-324 and disease progression in CRC patients, we probed for and analyzed probable correlations between the expression levels of SOD2 in stage I to stage IV, and metastatic CRC patients from the Taipei Medical University - Shuang Ho Hospital CRC cohort (n = 118). Our IHC staining data demonstrate that relative to its expression in the normal colorectal tissue samples, the expression of SOD2 in the CRC tissues is significantly increased as the disease progresses from stage I to stage IV (stage II: 2.2-fold, $p < 0.05$; stage III: 3.1-fold, $p < 0.01$; stage IV: 4.4-fold, $p < 0.001$); similarly, an estimated 2.4-fold increase was observed in SOD2 expression in the metastatic disease group, compared to the normal group ($p < 0.05$) (**Figures 3A** and **3B**). Having established a positive correlation between SOD2 expression, disease progression and metastasis (**Figures 3A** and **3B**), as well as corroborated the inverse correlation between SOD2 and hsa-miR-324 expression in CRC by using the TCGA colon cancer (COAD) dataset (n = 234, $\sigma = 0.695$, $p = 0.048$) (**Figure 3C**), we then evaluated the prognostic potential of SOD2 (n = 315) and hsa-miR-324-5p (n = 250) in CRC patients based on the TCGA COAD cohort using the Kaplan-Meier (KM) survival plot. Dichotomization of gene expression into high or low in the cohort was based on the median value of hsa-miR-324-5p or SOD2 expression. Patients with low SOD2 expression (< 12.07; n = 158; 5-year OS rate = 63.50%; 10-year OS rate = 51.0%) exhibited a 7.25 - 26.0% (1.1 - 2.0-fold) survival advantage over the high

Peer-reviewed version available at Cancers 2018, 10, 269; doi:10.3390/cancers10080269

SOD2 expression group (≥ 12.07; n = 157; 5-year OS rate = 56.25%; 10-year OS rate =25.0%) (**Figure 3D**). In parallel analyses, patients with high hsa-miR-324-5p expression (≥ 3.70; n = 124) exhibited 5- and 10-year OS rates of 52.5% and 43.75% respectively, while for the low hsa-miR-324-5p group (< 3.70; n = 126), the 5- and 10-year OS rates were 68.75% and 36.5%, revealing a time-dependent influence of hsa-miR-324-5p on the OS of CRC patients. Taken together, those findings do indicate that aberrant expression of SOD2 correlates with disease progression and the SOD2-induced down-regulation of hsa-miR-324 facilitates poor prognosis, while suggesting the molecular targetability of SOD2 and potential therapeutic utility of hsa-miR-324-5p in advanced stage and metastatic CRC patients.

3.4. 4-AAQB inhibits the viability and/or proliferation of wide-type and side-population human colorectal carcinoma cells.

Furthermore, we investigated the pharmacological targetability of the SOD2-enriched CRC cells, by evaluating the effect of 4-AAQB (**Figure 4A**) on the viability and proliferation of the CRC wild-type or sorted side-population (SP) cells, against the background of 4-AAQB bioinformatics-based predicted health benefits in several human systems, with highest (~ 99%) health effects in gastrointestinal system, which includes the colon and rectum (**Supplementary Figure 1**). Treatment with 2.5 - 12.5 μM 4-AAQB significantly suppressed the cell viability of DLD-1 or HCT116 cells in a dose-dependent manner, and with 24 h IC_{50} of 7.82 μM or 11.25 μM, respectively (**Figure 4B**). More importantly, considering the clinical relevance of CSC- targeting in effective anticancer therapy, we demonstrated that exposure to 2.5 μM, 5 μM, 7.5 μM or 10 μM 4-AAQB reduced the proportion of DLD-1 SP cells by 4.2% ($p < 0.01$), 7.4% ($p < 0.001$), 8.4% ($p < 0.001$), or 8.9% ($p < 0.001$), compared

Peer-reviewed version available at Cancers 2018, 10, 269; doi:10.3390/cancers10080269

to 6.4% by 100 µM verapamil, which specifically inhibits the Hoechst dye-extruding potential of the ATP-binding cassette (ABC) membrane transporter. For the HCT116 SP cells treated with 2.5 µM, 5 µM, 7.5 µM or 10 µM 4-AAQB, we observed 3.1% ($p < 0.001$), 3.6% ($p < 0.001$), 4.1% ($p < 0.001$), or 4.4% ($p < 0.001$) reduction, respectively, in comparison with 1.8% by 100 µM verapamil (**Figure 4C**). Additionally, we observed marked reduction in SP cell number (**Figure 4D**), as well as significant cell death and dysmorphism in cultured DLD-1 or HCT116 SP cells exposed to 10 µM 4-AAQB compared to the untreated control group; interestingly, 4-AAQB exhibited no significant inhibitory effect on the viability and/or proliferation of the non-tumor colon cell line, CRL-1831 (**Figure 4E**). This data indicates that 4-AAQB inhibits the viability and/or proliferation of human colorectal carcinoma wide-type and side-population cells, as well as corroborates the findings of our previously published work (8).

3.5. The anticancer effect of 4-AAQB, akin to SOD2-silencing, is mediated by hsa-miR-324 and associated with EMT- and cell-death-related molecular changes in colorectal cancer SP cells.

Investigating the molecular mechanism underlying the observed inhibitory effect of 4-AAQB in the SOD2-rich CRC SP cells, which serve as *in vitro* CRC-SC models, the results of our western blot analyses demonstrate that exposure to 5 - 10 µM 4-AAQB significantly down-regulates the expression level of SOD2, N-cadherin, vimentin, c-Myc and Bcl-xL proteins, while up-regulating the expression of E-cadherin and Bax in the DLD-1 or HCT116 SP cells (**Figure 5A** and **5B**). Similarly, in parallel assays, transient transfection of the DLD-1 SP cells with short interfering RNA specifically targeting SOD2 (siSOD2) resulted in the co-suppression

Peer-reviewed version available at Cancers 2018, 10, 269; doi:10.3390/cancers10080269

of SOD2, N-cadherin and Bcl-xL protein expression, while conversely enhancing E-cadherin and Bax protein expression levels (**Figure 5C).** Consistent with **Figure 5C**, the semi-quantitative analyses of E-cadherin, N-cadherin, SOD2, Bax, and Bcl-xl protein expression, as well as the Bax/Bcl-xL ratio in DLD-1siSOD2 cell line by RT-PCR exhibited similar expression profile (**Figure 5D**). Both the 4-AAQB and siSOD2-mediated proteomic and transcriptomic profile revealed an increase in the Bax/Bcl-xL ratio. Furthermore, using the RT-PCR, we demonstrated that DLD-1 SP cells treated with 10 µM 4-AAQB exhibited significantly suppressed SOD2 mRNA expression, and conversely up-regulated hsa-miR-324-5p expression. These data do suggest that the anticancer effect of 4-AAQB, akin to SOD2-silencing, is mediated by hsa-miR-324 and associated with EMT- and cell-death-related molecular changes in the colorectal cancer SP cells, at both the transcript and protein levels.

3.6. hsa-miR-324-inducing 4-AAQB inhibits SOD2-mediated motility, invasiveness and clonogenicity of colorectal cancer SP cells.

Having established that 4-AAQB effectively elicits the up-regulation of hsa-miR-324 while down-regulating SOD2 expression, we further investigated the effect of 4-AAQB treatment on the motility and oncogenicity of CRC-SCs using the sorted DLD-1 or HCT116 SP cells. We demonstrated that compared to observed migration by the untreated cells, exposure to 5 - 10 µM 4-AAQB significantly attenuate the ability of the SP cells to migrate in a dose-dependent manner over a 24 h time-course (**Figure 6A**). At the 24 h time-point, the DLD-1 SP cells treated with 5 -10 µM 4-AAQB had lost ~20 - 29% migratory potential, while the HCT116 SP cells recorded 41 - 59% lag in migration, in comparison to observed migration by their untreated counterpart (**Figure 6B**). Similarly, 4-AAQB treatment elicited

Peer-reviewed version available at Cancers 2018, 10, 269; doi:10.3390/cancers10080269

significant reduction in the number of invaded DLD-1 SP (5 µM: 35%, $p < 0.05$; 10 µM: 60%, $p < 0.01$) or HCT116 SP (5 µM: 11%, p = non-significant; 10 µM: 31%, $p < 0.01$) cells (**Figure 6C** and **6D**). Morever, we observed that there was significantly attenuated capacity to form colonies in the 4-AAQB-treated SP cells, in comparison to the untreated SP cells (**Figure 6E** and **6F**). These results indicate that 4-AAQB effectively inhibits the SOD2-mediated motility, invasiveness and clonogenicity of CRC SP cells.

3.7. 4-AAQB suppresses the cancer stem cell-like phenotype of colorectal cancer cells.

In parallel assays to confirm the inhibitory effect of 4-AAQB on CRC-SCs, after formation of primary colonospheres by wild-type DLD-1 or HCT116 cells cultured in stem cell media, we demonstrated marked dose-dependent attenuation of the viability and proliferative ability of the formed primary DLD-1 or HCT116 colonospheres when treated with 5 µM (DLD-1: 88% attenuation, $p < 0.05$; HCT116: 84% attenuation, $p < 0.01$), or 10 µM (DLD-1: 97% attenuation, $p < 0.05$; HCT116: 98.6% attenuation, $p < 0.001$) of 4-AAQB (**Figure 7A**). Since at the core of CRC cell resistance to chemotherapeutics, metastatic disease progression and tumor recurrence lies the characteristic CSC ability to regenerate all facets of the original/primary tumor and drive malignantization (21, 22), we examined if and how 4-AAQB affects the colonosphere-forming ability of single cell solutions derived from dissociated primary colonospheres and cultured in stem cell media (recapitulating CRC-SC self-renewal) in the presence of 5 - 10 µM 4-AAQB. We demonstrated that 4-AAQB significantly inhibited the self-renewal capacity of the DLD-1 (5 µM: 69% inhibition, $p < 0.01$; 10 µM: 90% inhibition, $p < 0.01$) or HCT116 (5 µM: 61% inhibition, $p <$

Preprints (www.preprints.org) | NOT PEER-REVIEWED | Posted: 13 July 2018 doi:10.20944/preprints201807.0223.v1

Peer-reviewed version available at Cancers 2018, 10, 269; doi:10.3390/cancers10080269

0.05; 10 µM: 80% inhibition, $p < 0.01$) primary colonospheres (**Figure 7B**). We further demonstrated that the quantitative and qualitative attenuation of DLD-1 or HCT116 colonosphere formation positively correlates with pronounced suppression of the nuclear expression of the pluripotency transcription factors, OCT4 and SOX2, in a dose-dependent manner (**Figure 7C**). These data indicate that 4-AAQB efficaciously suppresses the CSC-like phenotype, including the proliferation and self-renewal of CRC cells, *in vitro*.

3.8. 4-AAQB attenuate resistance to FOLFOX and reduce the tumorigenicity of colorectal cancer cells by suppressing SOD2 and up-regulating hsa-miR-324-5p expression, in vivo.

Since our team is practice-oriented, we pre-clinically probed for the translational relevance of our *in vitro* findings by assessing the *in vivo* effect of 4-AAQB and/or FOLFOX on the growth of CRC cells in the BALB/c mice (average body weight, 22.5±3.74 g) xenograft model. Results of our tumor xenograft assays showed by end of week 6, the tumors grown in mice inoculated with untreated DLD-1 cells ($n = 5$) were numerically more and much larger than those in mice treated with FOLFOX ($n = 5$, $p < 0.01$), 4-AAQB ($n = 5$, $p < 0.001$) or combination of 4-AAQB and FOLFOX ($n = 5$, $p < 0.001$), in descending order of degree (**Figure 8A** and **8B**). Macro-anatomically, The average weight of the tumors resected from the 4-AAQB- and combination-treated mice were significantly lesser than that of the FOLFOX- treated or untreated control mice (4-AAQB *vs* control: 334.3 ± 79.4 mg *vs* 3674.1 ± 593.1 mg, $p < 0.001$; Combination *vs* control: 282.6 ± 46.8 mg *vs* 3674.1 ± 593.1 mg, $p < 0.001$; FOLFOX *vs* control: 459.3 ± 57.9 mg *vs* 3674.1 ± 593.1 mg, $p < 0.01$) (**Figure 8A** and **8B**), indicating that the xenograft

Preprints (www.preprints.org) | NOT PEER-REVIEWED | Posted: 13 July 2018 doi:10.20944/preprints201807.0223.v1

Peer-reviewed version available at Cancers 2018, 10, 269; doi:10.3390/cancers10080269

tumor growth was significantly inhibited by 4-AAQB alone or in combination with FOLFOX, compared with the FOLFOX- treated or untreated group. Additionally, while the mean body weight of 4-AAQB - or dual agent- treated tumor-inoculated mice was stable, we observed a slight increase (~ 2g) in those treated with FOLFOX, as well as in the untreated control group (~ 4g) by end of week 6 (**Figure 8C**). The observed increase in body mass in the untreated and FOLFOX-treated littermates were however statistically insignificant, and all mice (n = 5/treatment regimen) exhibited normal feeding habit and motor activity. Finally, and interestingly, we demonstrated robust reciprocity in the differential expression of SOD2 and hsa-miR-324-5p in the tumors resected from the xenograft mice in all treatment groups, using the RT-PCR (**Figure 8D**). We observed statistically significant moderate ($p < 0.01$), mild ($p < 0.05$), or strong ($p < 0.001$) increase in the expression of hsa-miR-324-5p in mice treated with 4-AAQB alone, FOLFOX alone or 4-AAQB+FOLFOX combination, respectively (**Figure 8D**). Those results indicate that 4-AAQB is non-toxic to non-cancerous tissues (also see **Supplementary Figure 2**), and that alone or in synergism with FOLFOX, 4-AAQB significantly inhibits CRC xenograft tumor growth, *in vivo*.

4. Discussion

In our previous work (8) on the role of 4-AAQB in CRC, we provided evidence that 4-AAQB exhibits potent antiproliferative and anti-CSC therapeutic effect in CRC. We showed that 4-AAQB effectively reverses or attenuates the resistance of cancer cells to 5-FU or FOLFOX anticancer therapy, thus, enhancing chemosensitivity, both *in vitro* and *in vivo*. Furthermore, we demonstrated that the JAK/STAT signaling pathway plays a vital role in the 4-AAQB-mediated suppression

Peer-reviewed version available at Cancers 2018, 10, 269; doi:10.3390/cancers10080269

of CRC-SCs, thus, projecting it as a putative therapeutic target in the CRC treatment. Thus, we concluded that the relatively novel phytoalexin, 4-AAQB, was as a potent therapeutic agent for single-agent or component of standard combination chemotherapy. With increased understanding of the epigenetic landscape in cancer pathologies there has been increased interest and investigation of an epigenetics-mediated multipronged targeted-therapy strategy in tackling the clinical challenge of primary or evolved required resistance (23-25).

In this present study, consistent with current knowledge that epigenetic modulation of genes is a critical mechanism underlying the CRC oncogenicity and disease progression, as well as the development of resistance to chemotherapeutics, we demonstrate a novel and previously undocumented epigenetic-based mechanism of 4-AAQB therapeutic activity in CRC, involving the down-regulation of tumor-promoting SOD2 by the suppressor ncRNA, hsa-miR-324-5p. This negative epigenetic modulation of SOD2 was shown to be associated with the converse enrichment of hsa-miR-324 and through the interaction of the 3'-UTR of SOD2 mRNA to the 5'-UTR of hsa-miR-324 (**Figures 1 and 2**). Located on chromosome 6 (6q25.3 region) and resident in the mitochondrial matrix, the human homotetrameric SOD2 consists of four Mn^{3+}-harboring sub-units, catalyzes the disproportionation of free radical superoxides to O_2 and H_2O_2, and lowers cell susceptibility to oxidative injury in a genotoxic condition (12, 13). In most of the early documentations, SOD2 was implicated as a tumor suppressor (26), however, more recently, there is accruing evidence that of the oncogenic/tumor-promoting role of SOD2 (13-15). Consistent with the later, in this study we demonstrated the oncogenic role of the aberrant expression of SOD2 in CRC, as evidenced by its ability to facilitate metastatic disease progression through the repression of hsa-miR-324 (**Figure 3**). In addition, we also

showed that 4-AAQB inhibits the viability and/or proliferation of human CRC SP cells in a hsa-miR-324-mediated manner, with associated attenuation of the SOD2-facilitated EMT and enhanced cell-death in the SP cells (**Figures 4 and 5; Supplementary Figure 1**). These findings are consistent with the demonstrated suppression of the invasion and migration of hepatocellular carcinoma (HCC) cells by hsa-miR-324-5p-induced down-regulation of the specificity protein 1 (SP1) and E26 transformation-specific protein 1 (ETS1) (27), where decreased SP1 binding to the SOD2 promoter inhibits the constitutive activation of SOD2 in breast cancer cells (13), since the proximal promoter that mediates the transcription of SOD2 is TATA-less and contains binding sites for several transcription factors, including ETS1 and SP1. It is of therapeutic relevance that the hsa-miR-324-inducing 4-AAQB inhibits the SOD2-mediated motility, invasiveness and clonogenicity of colorectal cancer SP cells (**Figure 6**).

Like most malignancies, CRC is a SC-driven pathology, characterized by the presence of a sub- or side-population within the tumor bulk which are characteristically quiescent, phenotypically ALDH+, functionally capable of self-renewal, and underlie innate or acquired insensitivity to chemotherapy, metastasis and disease recurrence (28, 29). The targeting and killing of these CSC-like SP cells by 4-AAQB is posited as a rational and efficacious therapeutic approach as it eliminates the quiescent, slowly-dividing, and characteristically therapy-resistant tumor-initiating (and maintaining)-cells, alongside the sensitive rapidly-dividing non-SP cells. Consistent with this, we provided evidence that 4-AAQB in a dose-dependent manner, effectively targets the primary colonospheres and subsequent generations of colonospheres, recapitulating the pharmacological inhibition of

CRC-SC-related self-renewal or propagation, with associated attenuation of the expression of critical pluripotency transcription factors (**Figure 7**).

Understanding that self-renewal, a vital property of the CSC-like SP cells, is associated with the facilitation and maintenance of the proliferative capacity of cancerous cells, makes the clinical implication of our data apparent, as it highlights the putative ability of 4-AAQB to negatively modulate oncogenic self-renewal signaling, thus enhancing the sensitivity of malignant cells to chemotherapeutics, altering their survival strategies, limiting tumorigenesis and/or oncogenicity, and apparently impeding disease recurrence (30). In *in vivo* validation of our *in vitro* findings, we confirmed that 4-AAQB alone or in synergism with FOLFOX reduce the tumorigenicity of CRC cells by suppressing SOD and up-regulating hsa-miR-324 expression, *in vivo* (**Figure 8**). This is clinically-relevant and important not only because it is to the best of our knowledge, the first demonstration of an hsa-miR-324-5p-mediated anticancer activity of 4-AAQB in CRC, but also because despite advances in anticancer therapy, resistance to chemotherapy remains a great challenge in the long-term management of incurable metastatic disease and subsequently contributes to cancer-related mortality. FOLFOX is the therapeutic mainstay in postoperative CRC patients, having been shown in several trials to contribute to increased progression-free (PFS) and overall (OS) survival, with response rates as high as 50%, however, resistance to FOLFOX does occur because of its reduced intracellular entry or enhanced efflux from the CRC cells. ABC-type multi-drug resistance (MDR) transporters or copper-transporting p-type ATPases (reviewed in 31). In the light of this, we showed in addition that 4-AAQB enhances the sensitivity of CRC cells to the standard of care FOLFOX, and significantly

Peer-reviewed version available at Cancers 2018, 10, 269; doi:10.3390/cancers10080269

potentiate the anticancer effect of FOLFOX in the murine CRC xenograft models (**Figure 8; Supplementary Figure 2**).

Ranking as the third most common cancer and the fourth cause of cancer-related deaths worldwide, CRC remains a major health problem. FOLFOX, comprising of folinate (leucovorin), fluorouracil (5FU) and oxaliplatin is currently the drug of choice for patients with CRC, however some patients are non-responsive or develop insensitivity to FOLFOX, resulting in treatment failure and consequently, tumor progression, thus, necessitating a therapeutic approach with enhanced efficacy. This present study provides evidence that 4-AAQB alone or by synergistically interacting with FOLFOX, exhibits enhanced ability to kill CRC cells, inducing marked apoptosis via an epigenetically-modulated pathway. Mechanistically, hsa-miR-324-mediated inhibition of the SOD2-activated oncogenicity and cancer stem cell-like phenotype of CRC cells is a probable critical component of our observed 4-AAQB - FOLFOX anticancer synergism.

Interestingly, corroborating the critical role of epigenetic alterations in the unrestrained growth, invasion, colonization and acquired resistance of cancerous cells (16 - 20), we validated the reciprocal suppression of the pro-tumorigenic and pro-metastatic SOD2 and suppressor miR, hsa-miR-324 *ex-vivo*, showing that the expression of hsa-miR-324 levels in the resected tumor tissue from 4-AAQB- and/or FOLFOX- treated mice was significantly up-regulated, while conversely that of SOD2 was reduced markedly, compared to the untreated group (**Figure 8**). Overall, the data demonstrates that the hsa-miR-324/SOD2 signaling axis is a putative novel therapeutic target, and a potential prognostic marker in patients with CRC.

Put together, this present study uncovers a novel mechanistic underlining for the therapeutic effect of 4-AAQB or in combination with FOLFOX in the activation of

Peer-reviewed version available at *Cancers* **2018**, *10*, 269; doi:10.3390/cancers10080269

cell death signals, attenuation of CSC-like phenotypes, and induction of apoptosis in the CRC cells. Akin to the single-agent therapy, the pharmacological synergism involves multiple mechanisms as summarized in the **Schematic abstract**. The enhanced cytotoxicity of 4-AAQB - FOLFOX dual-agent therapy is clinically-relevant. We propose that SOD2-enrichment in the CRC cells, accentuates mitochondrial biogenesis, activates the intracellular anti-oxidative machinery, alleviate oxidative stress, and enhances the maintenance of the CSC-like phenotype as well as acquisition of resistance to chemotherapeutic agents, by functional suppression of hsa-miR-324-5p expression and/or activity, however, exposure to 4-AAQB induces the re-expression of hsa-miR-324-5p, attenuates SOD2 expression, and sensitizes the CSC-like SP cells in CRC to FOLFOX therapy. Thus, we propound a novel perspective on the putative roles of 4-AAQB as a hsa-miR-324-mediated CSC- targeting small molecule inhibitor of SOD2 in CRC, *in vitro* and *in vivo*.

Authors' contributions

O.A.B and C.K.Y: Project conception, Experimental design, Collation and/or assembly of data, Data analysis and interpretation, Computational biology, Manuscript writing. W.H.C, K.T.K: Collation and/or assembly of data, Data analysis and interpretation. D.T.W.T, C.C.H, Y.M.T, L.D: Data assembly and analysis. C.T.Y, W.H.L: Experimental design, Provision of useful research insight and essential reagents, Administrative oversight. All authors read and approved the final submitted version.

Acknowledgments

This work was supported by National Science Council of Taiwan [MOST-103-2113-M-324-001-MY2, MOST-103-2811-M-324-001 to Y.M.T], [MOST-105-2320-B-038-054 to W.H.L]; and the Taipei Medical University [102TMU-SHH-02 to W.H.L, 105TMU-SHH-15, 106-FRP-04 to J.T.T].

Peer-reviewed version available at Cancers 2018, 10, 269; doi:10.3390/cancers10080269

Disclosure Statement

The authors have declared no conflict of interest.

Peer-reviewed version available at Cancers 2018, 10, 269; doi:10.3390/cancers10080269

5. References

1. Torre L.A. et al. (2015) Global cancer statistics, 2012. CA Cancer J Clin., 65(2):87-108.
2. Siegel R.L. et al (2017) Colorectal cancer statistics, 2017. CA Cancer J Clin., 67(3):177-193.
3. Brenner H. et al (2014) Colorectal cancer. Lancet, 383(9927):1490-1502.
4. Favoriti P. et al. (2016) Worldwide burden of colorectal cancer: a review. Updates Surg., 68(1):7-11.
5. Valachis A. et al. (2012) Financial relationships in economic analyses of targeted therapies in oncology. J Clin Oncol., 30(12):1316-20
6. Marin J.J. et al (2012) Chemoprevention, chemotherapy, and chemoresistance in colorectal cancer. Drug Metab Rev., 44: 148–172.
7. Boman B.M. et al. (2008) Human Colon Cancer Stem Cells: A New Paradigm in Gastrointestinal Oncology. J Clin Oncol., 26(17): 2828-2838
8. Chang T.C. et al (2015) 4-Acetylantroquinonol B inhibits colorectal cancer tumorigenesis and suppresses cancer stem-like phenotype. Toxicol Appl Pharmacol., 288(2):258-68.
9. Iorio M.V. et al. (2012) MicroRNA dysregulation in cancer: diagnostics, monitoring and therapeutics. A comprehensive review. EMBO molecular medicine , 4: 143–159
10. Zeng W. et al. (2015) Predictive power of circulating miRNAs in detecting colorectal cancer. Tumour Biol., 36(4): 2559–2567.
11. Leufkens A.M. et al. (2012) Biomarkers of oxidative stress and risk of developing colorectal cancer: a cohort-nested case-control study in the European Prospective Investigation into Cancer and Nutrition. Am J Epidemiol., 175(7):653-63.
12. Demicheli V. et al. (2016) Mechanism of the Reaction of Human Manganese Superoxide Dismutase with Peroxynitrite: Nitration of Critical Tyrosine 34. Biochemistry, 55(24):3403–3417.

Peer-reviewed version available at Cancers 2018, 10, 269; doi:10.3390/cancers10080269

13. Hempel N. et al. (2011) Manganese superoxide dismutase (Sod2) and redox-control of signaling events that drive metastasis. Anticancer Agents Med Chem., 11(2):191-201.

14. Termini L. et al. (2011) Deregulated expression of superoxide dismutase-2 correlates with different stages of cervical neoplasia. Dis Markers., 30(6):275–81.

15. Chang B. et al. (2016) SOD2 deregulation enhances migration, invasion and has poor prognosis in salivary adenoid cystic carcinoma. Sci Rep., 6:25918.

16. Berdasco M. et al. (2010) Aberrant Epigenetic Landscape in Cancer: How Cellular Identity Goes Awry. Dev Cell., 19(5):698-711

17. Dvinge H. et al. (2013) The shaping and functional consequences of the microRNA landscape in breast cancer. Nature. , 497(7449):378-82.

18. Wang R.T. et al. (2014) Decreased expression of miR216a contributes to non-small-cell lung cancer progression. Clin Cancer Res., 20:4705–16.

19. Li J.H. et al (2014) starBase v2.0: decoding miRNA-ceRNA, miRNA-ncRNA and protein–RNA interaction networks from large-scale CLIP-Seq data. Nucleic Acids Research, 42(D1): D92–D97.

20. Bellucci M. et al. (2011) Predicting protein associations with long noncoding RNAs. Nat Methods. , 8(6):444–5.

21. O'Brien C.A. et al. (2010) Cancer stem cells and self-renewal. Clin Cancer Res., 16(12):3113-20.

22. Medema J.P. (2017) Targeting the Colorectal Cancer Stem Cell. N Engl J Med., 377(9):888-890

23. Jones P.A. et al. (2016) Targeting the cancer epigenome for therapy. Nat Rev Genet. , 17(10):630-641

24. van Engeland M. et al. (2011) , Derks S, Smits KM, Meijer GA, Herman JG. Colorectal cancer epigenetics: complex simplicity. J Clin Oncol., 29(10):1382-91.

25. Crea F. et al. (2011) Epigenetics and chemoresistance in colorectal cancer: an opportunity for treatment tailoring and novel therapeutic strategies. Drug Resist Updat. , 14(6):280-96.

26. Bravard A. et al. (1992) SOD2: a new type of tumor-suppressor gene? Int J Cancer, 51(3):476-80.

27. Cao L. et al. (2015) MiR-324-5p Suppresses Hepatocellular Carcinoma Cell Invasion by Counteracting ECM Degradation through Post-Transcriptionally Downregulating ETS1 and SP1. PLoS ONE, 10(7): e0133074.

28. Raha D. et al. (2014) The cancer stem cell marker aldehyde dehydrogenase is required to maintain a drug-tolerant tumor cell subpopulation. Cancer Res., 74(13): 3579–3590.

29. Huang E.H. et al. (2009) Aldehyde dehydrogenase 1 is a marker for normal and malignant human colonic stem cells (SC) and tracks SC overpopulation during colon tumorigenesis. Cancer Res., 69(8):3382–3389.

30. Borah A. et al. (2015) Targeting self-renewal pathways in cancer stem cells: clinical implications for cancer therapy. Oncogenesis, 4(11): e177.

31. Hammond W.A. et al. (2016) Pharmacologic resistance in colorectal cancer: a review. Ther Adv Med Oncol., 8(1):57-84.

Peer-reviewed version available at Cancers 2018, 10, 269; doi:10.3390/cancers10080269

Figure Legends

Fig. 1. SOD2 is aberrantly expressed in malignancies and correlates with the suppression of hsa-miR-324 expression. (A) Comparative analyses of the SOD2 expression levels in normal-cancer tissue pairs of the TCGA 14 cancer type - pancancer cohort dataset using the starBase v2.0 software algorithms. (B) SOD2 is up-regulated in colon and rectal adenocarcinoma, CRC samples compared to normal samples (fold change=1.05, student t-test p-value=0.59432). (C) Comparative analyses of the hsa-miR-324-5p expression levels in normal-cancer tissue pairs of the TCGA 14 cancer type - pancancer cohort dataset. (D) decreased levels of hsa-miR-324-5p in cancer compared to normal samples (fold change=0.26, student t-test p-value=1.03473e-13).

Fig. 2. SOD2 interacts with and is modulated by hsa-miR-324. (A) Crystal structure of the human manganese superoxide dismutase, PDB: 2ADQ. (B) The optimal secondary structure in dot-bracket notation with a minimum free energy (MFE) of -35.90 kcal/mol, *(upper panel)*. The RNAfold generated MFE secondary folding structure pattern of hsa-miR-324 *(lower panel, left)*. The hsa-miR-342 tertiary structure generated based on the secondary structure in dot-bracket notation *(lower panel, right)*. (C) Molecular docking showing the direct interaction between SOD2 and hsa-miR-324 with a shape complementarity/docking score of 14236, Atomic contact energy ACE of -33.40 and an approximate SOD2-hsa-miR-324 complex interface area of1896.30, using a root mean square distance, RMSD of 9 for the final docking. The 3D transformation data consisting of 3 rotational angles (38.44 20.02 216.62) and 3 translational parameters (-0.02 0.94 -1.95) applied on the ligand molecule, hsa-miR-324. (D) Representative western blot image *(left panel)* and quantitative graphical representation *(right panel)* of the effect of variations in hsa-miR-324 expression on the expression level of SOD2 protein. β-actin served as loading control. NC, negative control; OD, optical density; *p < 0.05, **p < 0.01, ***p <0.001

Preprints (www.preprints.org) | NOT PEER-REVIEWED | Posted: 13 July 2018 doi:10.20944/preprints201807.0223.v1

Peer-reviewed version available at Cancers 2018, 10, 269; doi:10.3390/cancers10080269

Fig. 3. Aberrant expression of SOD2 correlates with disease progression and SOD2-induced down-regulation of hsa-miR-324 facilitates poor prognosis. (A) Representative IHC images of differential SOD2 protein expression in non-tumor, stages I - IV and metastatic colon cancer tissue samples (n=118). (B) Box and whiskers graph of the expression (Q-score) of SOD2 in stages I - IV and metastatic colon cancer tissue samples, compared to its expression in normal tissues. (C) A bivariate fit of SOD2 and hsa-miR-324 gene expression using data from the TCGA Colon Cancer (COAD) cohort dataset, TCGA. COAD.sampleMap/HiSeqV2, based on the gene-level transcription estimates, as in log2(x+1) transformed RSEM normalized count. Kaplan-Meier plots of the (D) SOD2 and (E) hsa-miR-324 differential expression-based overall survival rates of same TCGA Colon Cancer (COAD) cohort. * $p < 0.05$, ** $p < 0.01$, *** $p < 0.001$

Fig. 4. 4-AAQB inhibits the viability and/or proliferation of human colorectal carcinoma side population cells. (A) The chemical structure of 4-Acetylantroquinonol B ($C_{26}H_{38}O_7$) with a molecular weight of 462.6 g/mol. (B) The inhibitory effect of 4-AAQB on the viability of DLD-1 *(left panel)* and HCT116 *(right panel)* colorectal cancer cell lines, using the SRB cytotoxicity assay. (C) Representative flow-cytometry dot plots of the dose-dependent attenuation of DLD-1 *(upper panel)* and HCT116 *(lower panel)* colorectal cancer side population cells by 4-AAQB, quantified by FACS analysis. Control, cells were incubated in Hoechst 33342 alone (serving as negative control); Verapamil, cells with Hoechst 33342 accumulation in the presence of 100µM verapamil (serving as positive control); 4-AAQB, cells with Hoechst 33342 accumulation in the presence of 2.5µM - 10 µM 4-AAQB. (D) Graphical representation of C. (E) Photomicrograph showing the morphological and quantitative changes in cultured 4-AAQB -treated CRL-1831 non-tumor colon cells, DLD-1 and HCT116 colorectal cancer SP cells, compared to their untreated control counterparts.

Fig. 5. The anticancer effect of 4-AAQB is mediated by hsa-miR-324 and consistent with EMT- and cell-death-related molecular changes in colorectal cancer SP cells. (A) 4-AAQB down-regulates N-cadherin, Vimentin, C-myc, SOD2

and Bcl-xl, but up-regulate E-cadherin and Bax. (B) Semi-quantitative analyses of E-cadherin, N-cadherin, SOD2 and the ratio of Bax and Bcl-xl protein expression in DLD1 and HCT116 cells treated with 4-AAQB. (C) SOD2 siRNA knockdown DLD1 show down-regulation of N-cadherin, with up-regulation of E-cadherin and Bax. (D) Semi-quantitative analyses of E-cadherin, N-cadherin, SOD2, Bax, Bcl-xl and the ratio of Bax and Bcl-xl transcript expression in siSOD2 DLD1 cell line by RT-PCR. *p <0.05, **p < 0.01, ***p < 0.001. (E) Graphical representation of the effect of 10 µM 4-AAQB treatment on SOD2 mRNA and hsa-miR-324 expression levels in DLD1 SP cells evaluated by RT-PCR. Statistical significance is indicated using * for CTL vs 4-AAQB, and δ for hsa-miR-324 vs SOD2. δδp < 0.01, ***p < 0.001; SP, side population cells; #1, siSOD2 clone 1; #2, siSOD2 clone 2.

Fig. 6. hsa-miR-324-inducing 4-AAQB inhibits the SOD2-mediated motility, invasiveness and clonogenicity of colorectal cancer SP cells. (A) Representative micrograph showing the dose-dependent effect of 4-AAQB on the migration of DLD1 and HCT116 SP cells at the 24h time-point, using the scratch-wound healing assays. (B) Histographs of the estimated wound closure or migration by DLD1 and HCT116 colorectal cancer SP cells exposed to 5 µM or 10 µM 4-AAQB, compared with the untreated control SP cells. (C) Micrographs and (D) histograms showing the dose-dependent reduction in number of invaded SP cells, after 4-AAQB treatment of DLD1 and HCT116 SP cells, as evaluated by the matrigel invasion assay. (E, F) Dose-dependent attenuation of clonogenicity after 4-AAQB treatment of DLD1 and HCT116 SP cells. Data are expressed as the mean ± S.E.M. and are representative of experiments performed thrice in triplicate. * p < 0.05, ** p < 0.01, *** p< 0.001.

Fig. 7. 4-AAQB suppresses the cancer stem cell-like phenotype of colorectal cancer cells. (A) DLD1 and HCT116 cells pre-treated with 5 or 10 µM 4-AAQB for 48 h exhibit decreased colonosphere size *(left panel)* and number *(right panel)* in both (A) primary and (B) secondary generation tumorspheres. (C) Treatment with 4-AAQB attenuated OCT4 and SOX2 immunoreactivity and inhibited their nuclear co-localization in DLD1- or HCT116-derived colonospheres using the

Preprints (www.preprints.org) | NOT PEER-REVIEWED | Posted: 13 July 2018 doi:10.20944/preprints201807.0223.v1

Peer-reviewed version available at Cancers 2018, 10, 269; doi:10.3390/cancers10080269

immunofluorescent (IFC) staining technique. Data are expressed as the mean ± S.E.M. and are representative of experiment performed thrice in triplicate.

Fig. 8. 4-AAQB alone or in synergism with FOLFOX reduces the tumorigenicity of colorectal cancer cells by suppressing SOD2 and up-regulating hsa-miR-324-5p expression, *in vivo*. (A) Colorectal cancer cell line, DLD1 cells were injected into the right flank of the animals at a concentration of 1×10^5 cells/100 µl PBS. One week after tumor injection, different treatment regimens were started. Photographs of tumor-bearing mice are shown (n = 5 each group) with treatment regimens labelled on the left-hand column. (B) Graphical representation of treatment-related fold change in tumor volume over time. The tumor volume of each group was measured each week using a calliper. Treatment started a week after tumor xenograft and lasted 5 weeks. (C) Correlation between different treatment regimens and cancer-associated body weight change. (D) Graphical representation of the effect of FOLFOX and/or 4-AAQB on SOD2 mRNA and hsa-miR-324 expression levels in the resected tumor tissue from treated mice (n = 5/each treatment regimen), compared to untreated group (n = 5), as evaluated by RT-PCR. Statistical significance is indicated using * for untreated vs treated, and δ for hsa-miR-324-5p vs SOD2. δδp < 0.01, δδδp < 0.001, *p <0.05, **p < 0.01, ***p < 0.001. untrt, untreated control

Schematic abstract. A pictorial summary of the anticancer therapeutic activity of 4-AAQB, alone or in combination with FOLFOX against CSCs in CRC cells. 4-AAQB inhibits the aberrant expression of SOD2 through the re-expression of hsa-miR-324-5p, negative modulation of pluripotency transcription factors, augmentation of the BAX/BCL-xL ratio and reprogramming of malignant colorectal cancer cells from the aggressive mesenchymal phenotype to a relatively benign epithelial phenotype, subsequently enhancing sensitivity of the cancer cells to conventional chemotherapy and facilitating better prognosis.

Peer-reviewed version available at Cancers 2018, 10, 269; doi:10.3390/cancers10080269

Supplementary Data:

Supplementary Figure 1. Bioinformatics-based systemic pharmacoanalyses reveal health effect of 4-AAQB. Predicted values of the health benefits of 4-AAQB is shown in several human systems, with highest (~ 99%) health effects in gastrointestinal system, which includes the colon and rectum, using the ACD/Labs 2.0 v5.0.0.184 platform.

Supplementary Figure 2. 4-AAQB dose determination and ADMET analyses for *in vivo* assays. (A) Bioinformatic computation of the physicochemical descriptors and prediction of ADME parameters, pharmacokinetic properties, drug-like nature and medicinal chemistry friendliness of 4-AAQB using the SwissADME platform. (B) Data showing the results of *in silico* drug safety/toxicity analysis on the pkCSM platform. Charts showing (C) the administration route and bioinformatics-based predicted lethality dose, LD in different species, and (D) Predicted values for oral acute toxicity hazard categories, OECD ranges, using the ACD/Labs 2.0 v5.0.0.184. ADMET, absorption, distribution, metabolism, excretion, and toxicity; OECD, Organisation for Economic Cooperation and Development; Cat., category

Preprints (www.preprints.org) | NOT PEER-REVIEWED | Posted: 13 July 2018 doi:10.20944/preprints201807.0223.v1

Peer-reviewed version available at Cancers 2018, 10, 269; doi:10.3390/cancers10080269

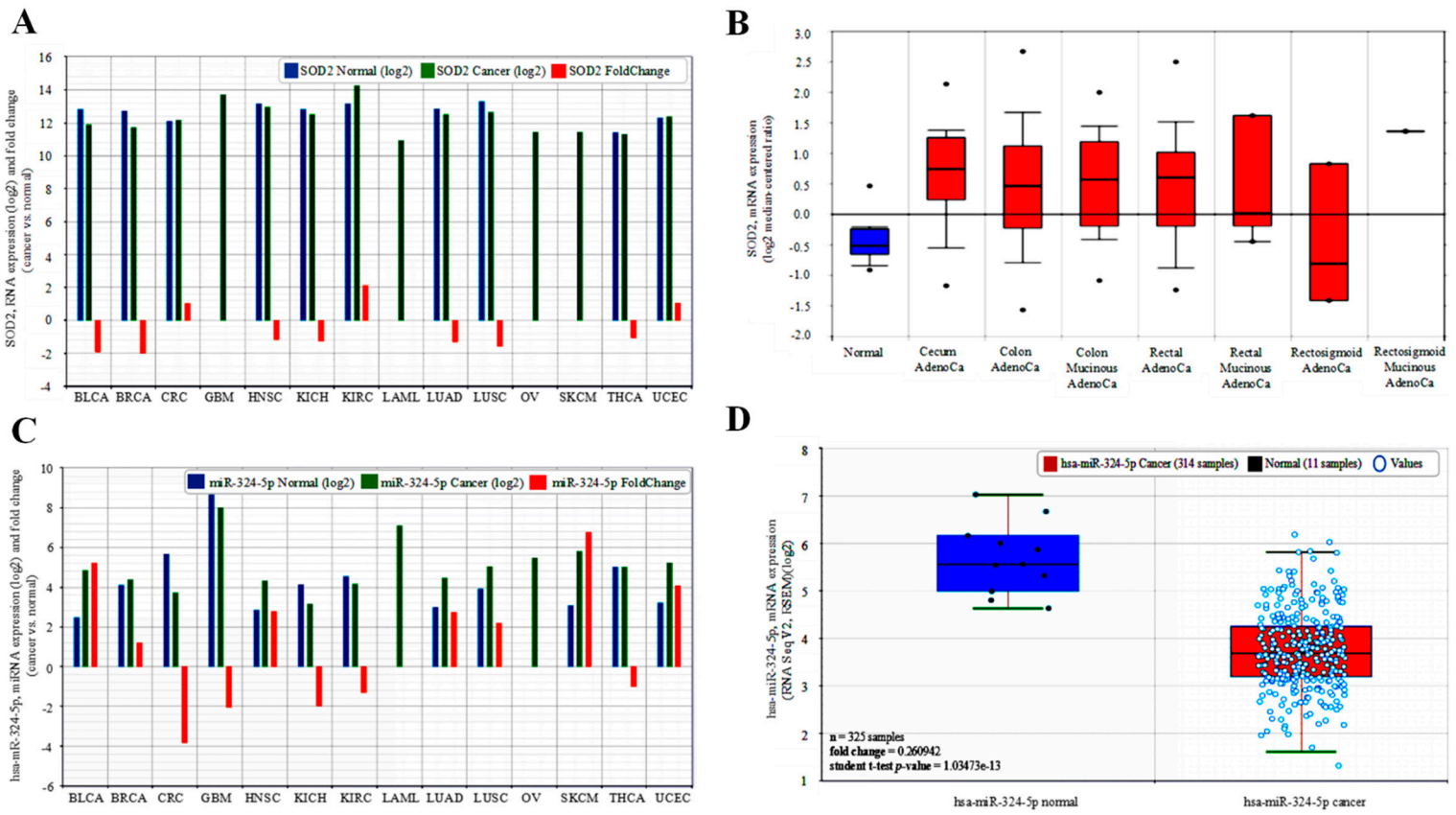

Figure 1

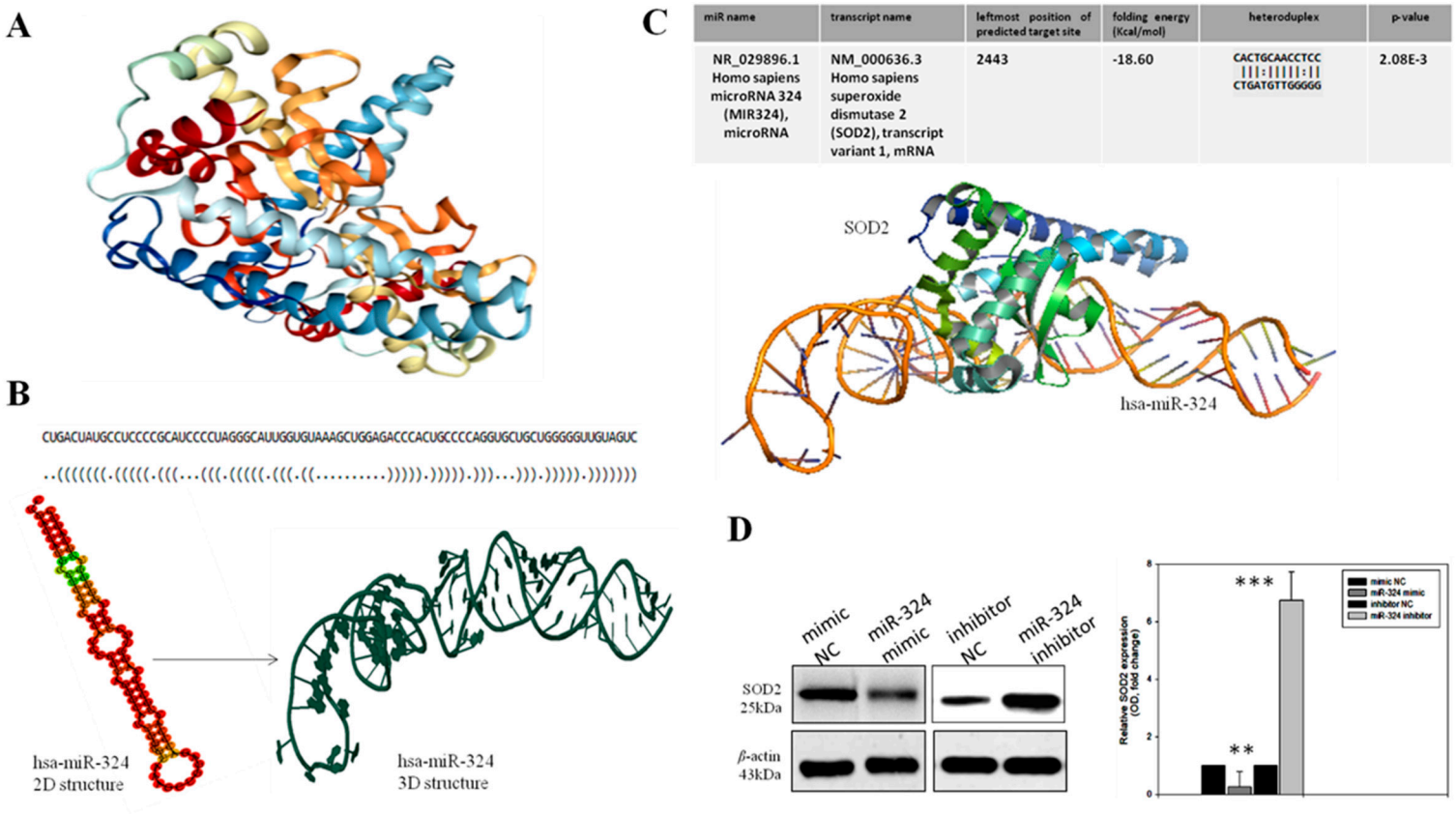

Figure 2

Preprints (www.preprints.org) | NOT PEER-REVIEWED | Posted: 13 July 2018 doi:10.20944/preprints201807.0223.v1

Peer-reviewed version available at Cancers 2018, 10, 269; doi:10.3390/cancers10080269

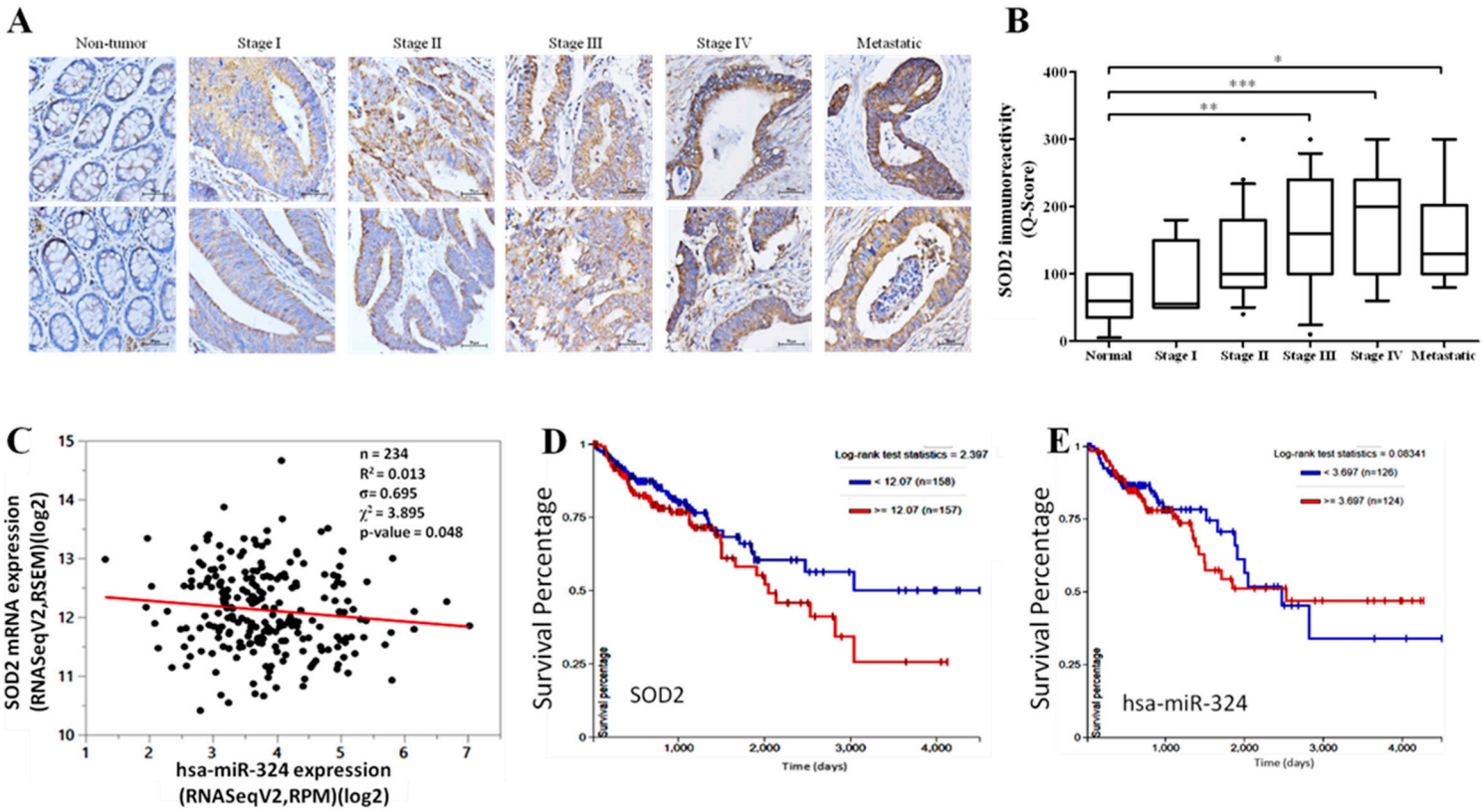

Figure 3

Preprints (www.preprints.org) | NOT PEER-REVIEWED | Posted: 13 July 2018 doi:10.20944/preprints201807.0223.v1

Peer-reviewed version available at Cancers 2018, 10, 269; doi:10.3390/cancers10080269

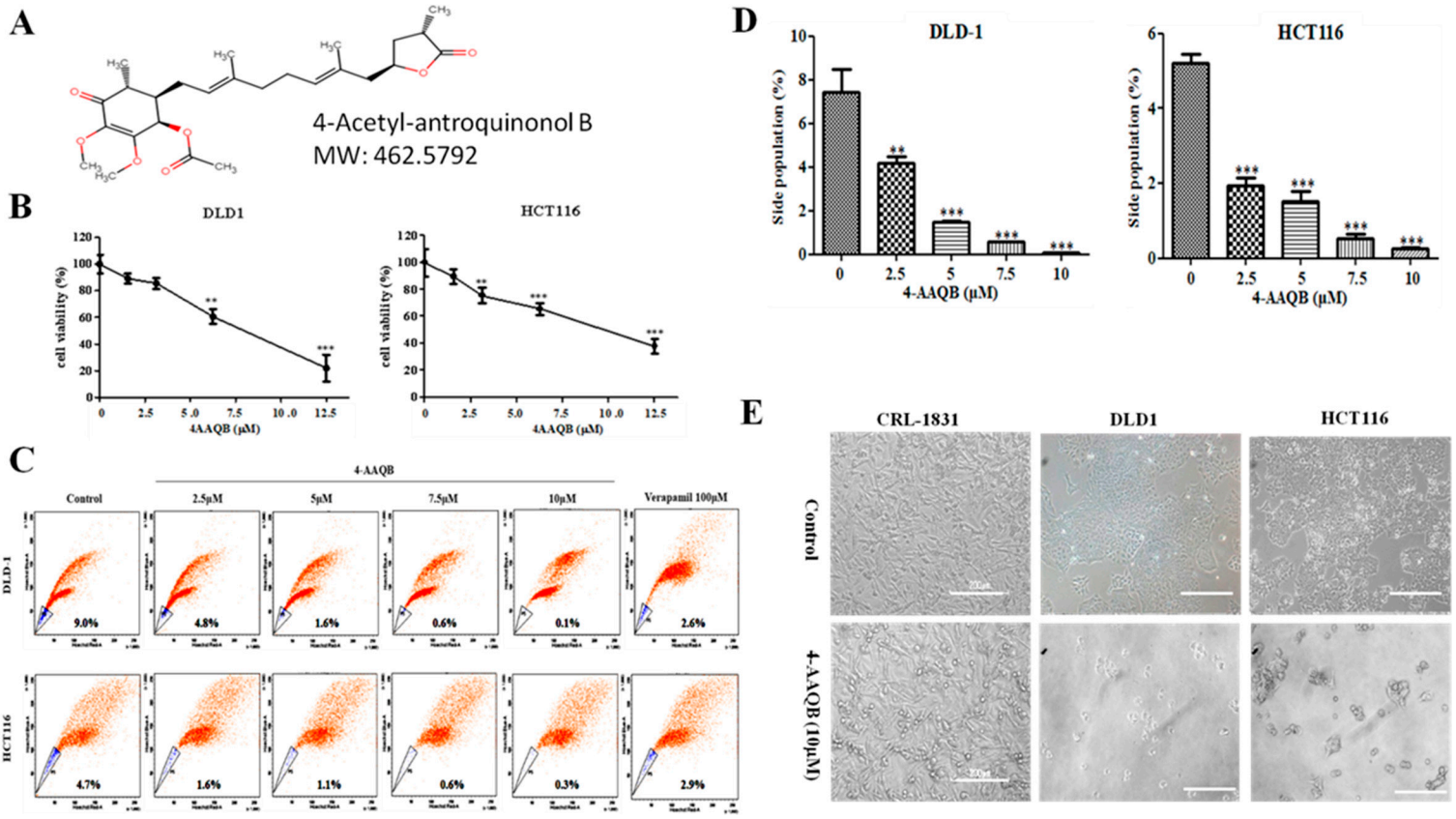

Figure 4

Preprints (www.preprints.org) | NOT PEER-REVIEWED | Posted: 13 July 2018 doi:10.20944/preprints201807.0223.v1

Peer-reviewed version available at Cancers 2018, 10, 269; doi:10.3390/cancers10080269

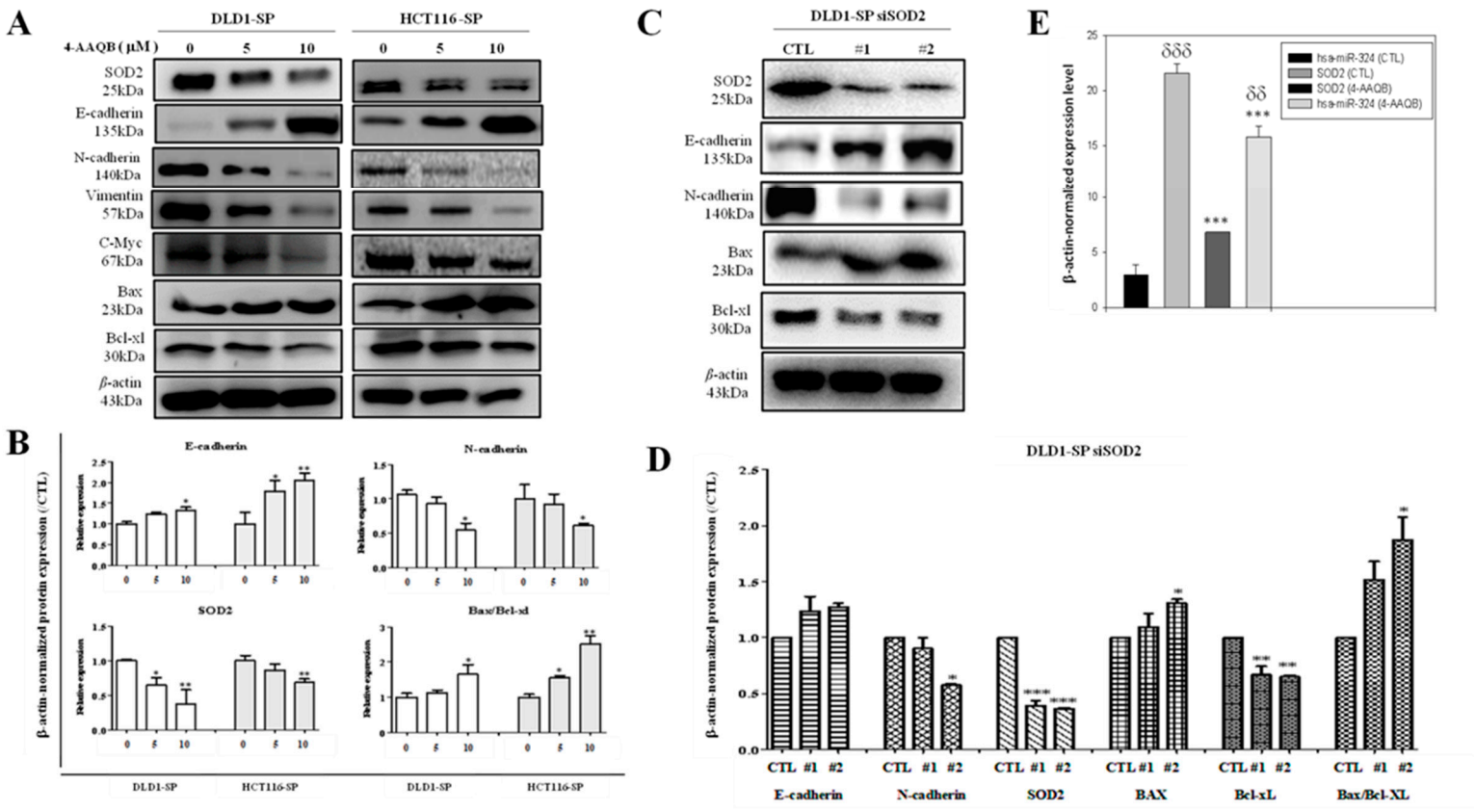

Figure 5

Preprints (www.preprints.org) | NOT PEER-REVIEWED | Posted: 13 July 2018 doi:10.20944/preprints201807.0223.v1

Peer-reviewed version available at Cancers 2018, 10, 269; doi:10.3390/cancers10080269

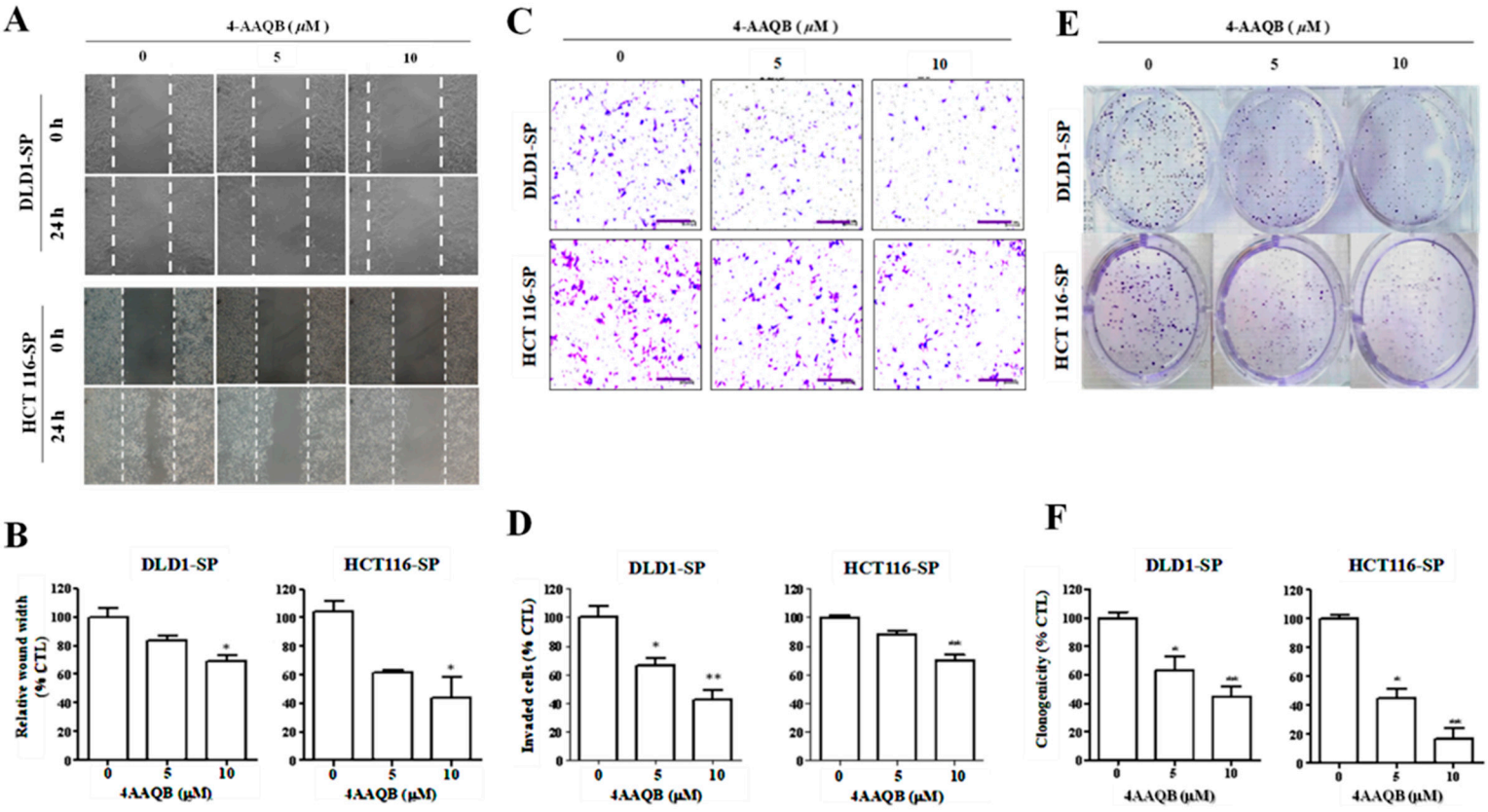

Figure 6

Preprints (www.preprints.org) | NOT PEER-REVIEWED | Posted: 13 July 2018 doi:10.20944/preprints201807.0223.v1

Peer-reviewed version available at Cancers 2018, 10, 269; doi:10.3390/cancers10080269

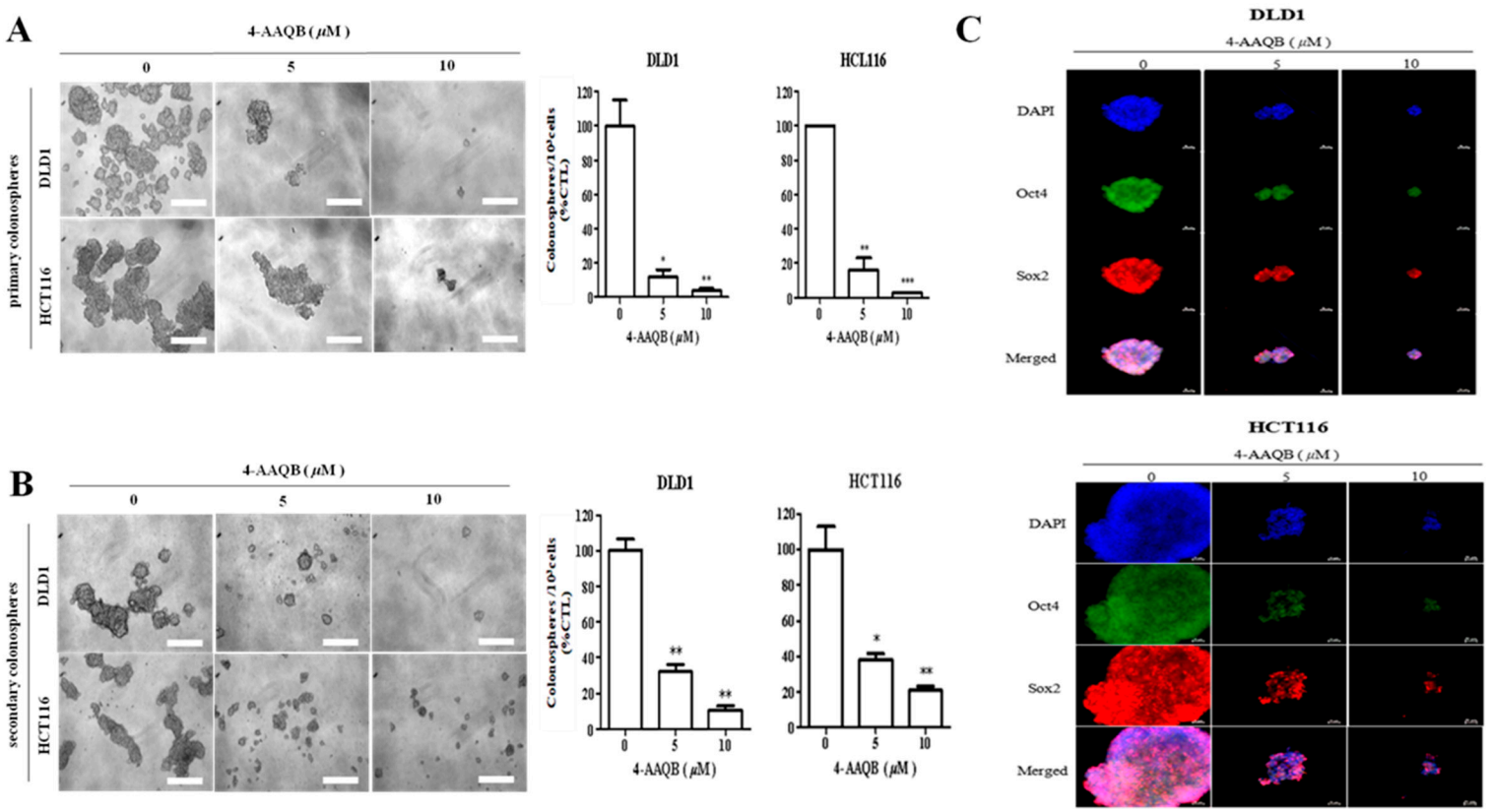

Figure 7

Preprints (www.preprints.org) | NOT PEER-REVIEWED | Posted: 13 July 2018 doi:10.20944/preprints201807.0223.v1

Peer-reviewed version available at Cancers 2018, 10, 269; doi:10.3390/cancers10080269

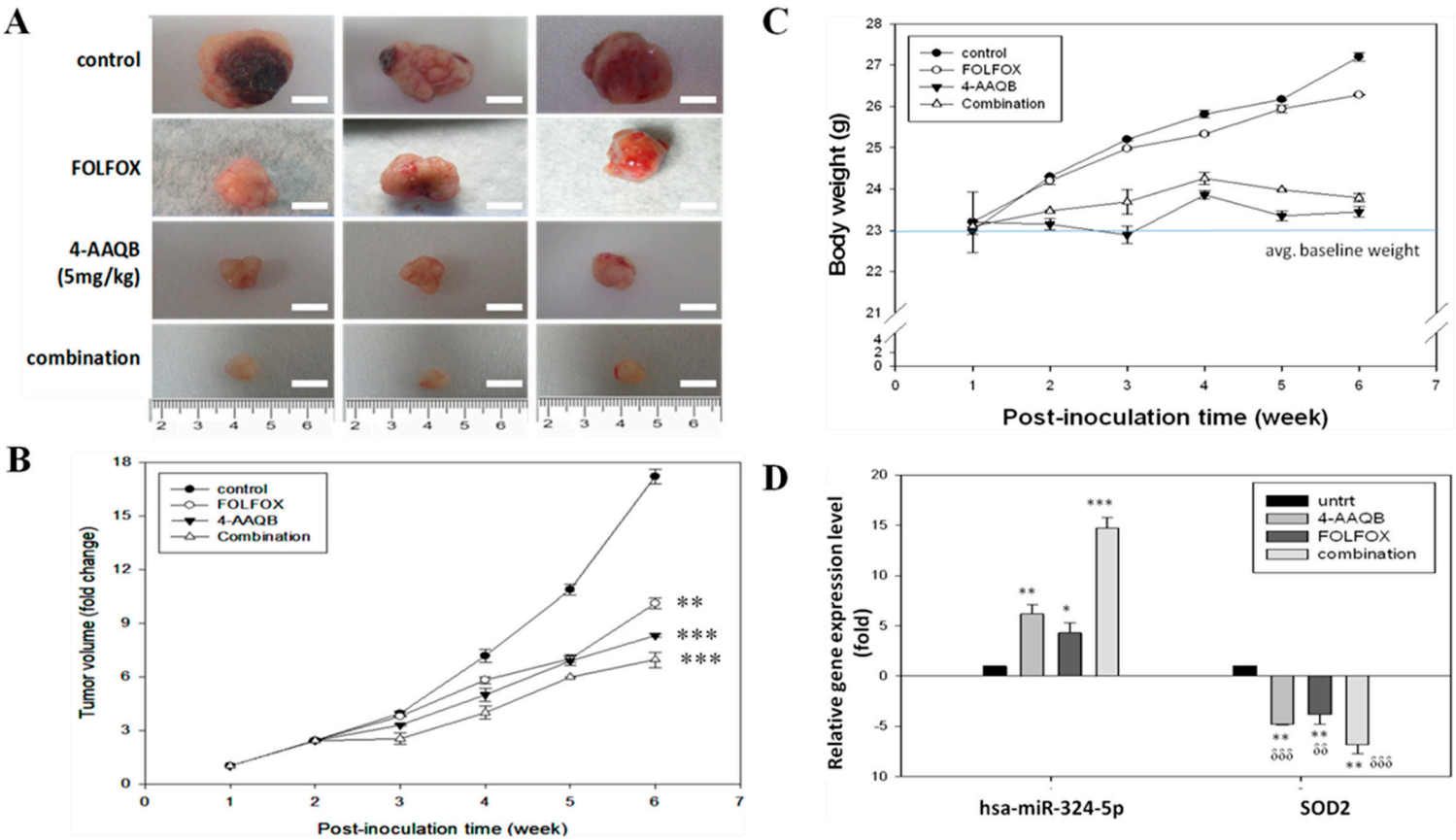

Figure 8